AD-A112 563 NAVAL RESEARCH LAB. WASHINGTON DC F/G 20/14
A SUMMARY OF PROPAGATION STUDIES UNDERTAKEN BY THE 1981 EXPEDIT--ETC(U)
MAR 82 J M GOODMAN, A J MARTIN
UNCLASSIFIED NRL-MR-4720 NL

1 OF 1
AD A
112563

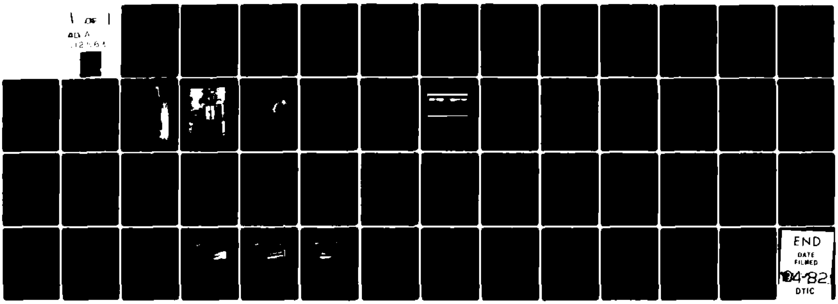

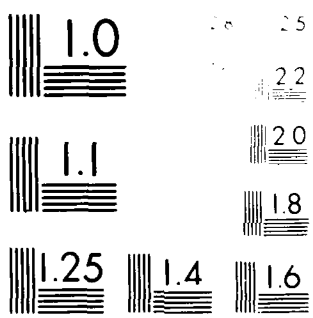
1.0
2.5
2.2
2.0
1.1
1.8
1.25
1.4
1.6

NRL Memorandum Report 4720

A Summary of Propagation Studies Undertaken by the 1981 Expedition of the USNS Hayes

J. M. GOODMAN AND A. J. MARTIN

Ionospheric Effects Branch
Space Science Division

March 30, 1982

This research was partially supported by NAVELEX.

NAVAL RESEARCH LABORATORY
Washington, D.C.

Approved for public release; distribution unlimited.

SECURITY CLASSIFICATION OF THIS PAGE (When Data Entered)

REPORT DOCUMENTATION PAGE	READ INSTRUCTIONS BEFORE COMPLETING FORM
1. REPORT NUMBER: NRL Memorandum Report 4720 — 2. GOVT ACCESSION NO.	3. RECIPIENT'S CATALOG NUMBER
4. TITLE (and Subtitle): A SUMMARY OF PROPAGATION STUDIES UNDERTAKEN BY THE 1981 EXPEDITION OF THE USNS HAYES	5. TYPE OF REPORT & PERIOD COVERED: Final report on one phase of a continuing NRL problem.
	6. PERFORMING ORG. REPORT NUMBER
7. AUTHOR(s): J.M. Goodman and A.J. Martin	8. CONTRACT OR GRANT NUMBER(s)
9. PERFORMING ORGANIZATION NAME AND ADDRESS: Naval Research Laboratory, Washington, DC 20375	10. PROGRAM ELEMENT, PROJECT, TASK AREA & WORK UNIT NUMBERS: 61153N; RR033-02-44; 0153-0-1; 0149-0-1/2; 0990-0-1
11. CONTROLLING OFFICE NAME AND ADDRESS: Office of Naval Research, Arlington, VA 22217	12. REPORT DATE: March 30, 1982
	13. NUMBER OF PAGES: 52
14. MONITORING AGENCY NAME & ADDRESS (if different from Controlling Office)	15. SECURITY CLASS. (of this report): UNCLASSIFIED
	15a. DECLASSIFICATION/DOWNGRADING SCHEDULE

16. DISTRIBUTION STATEMENT (of this Report)

Approved for public release; distribution unlimited.

17. DISTRIBUTION STATEMENT (of the abstract entered in Block 20, if different from Report)

18. SUPPLEMENTARY NOTES

This research was partially supported by NAVELEX under program element 64711N, task area X-1144-CC, NRL problem no. 1475-0-1.

19. KEY WORDS (Continue on reverse side if necessary and identify by block number)

UHF scintillation	Equatorial scintillation
Earth-space propagation	Maritime propagation effects
L-Band scintillation	Appleton anomaly

20. ABSTRACT (Continue on reverse side if necessary and identify by block number)

Between 1 January and 15 April 1981, investigators at the Naval Research Laboratory participated in comprehensive radiowave propagation studies in the American longitude zone using radio receivers installed aboard the US Naval Research Ship USNS Hayes (T-AGOR-16). Both UHF and L-band data were obtained using the transmissions from the Atlantic FLTSATCOM and from the existing complement of NAVSTAR/GPS

(Continued)

DD FORM 1473, 1 JAN 73 — EDITION OF 1 NOV 65 IS OBSOLETE

S/N 0102-014-6601

SECURITY CLASSIFICATION OF THIS PAGE (When Data Entered)

20 ABSTRACT (Continued)

satellites respectively. This report primarily describes the UHF scintillation data obtained during the Hayes expedition which covered geographic latitudes between 35° N and 50° S with considerable concentration in the Southern hemisphere. Preliminary study of the L-band data is underway.

Strong scintillation at 250 MHz was observed ($\geq$20dB) in the vast majority of nocturnal periods for which the magnetic dip angle (I) between 0° and ± 40°. This corresponds to roughly ± 30° in geomagnetic (centered dipole) latitude and about ± 23° dip latitude. This represents an expansion in the equatorial scintillation zone currently thought to apply to UHF scintillation and is thought to be circumstantially related to the enhanced solar activity during the period of observation. It also has implications vis-a-vis the maximum altitude achieved by plasma bubbles (electron density holes) which propagate vertically upward from their origin in the equatorial ionosphere and are mapped along field lines into the intermediate F region at higher latitudes. It also relates to the maximum poleward position of the anomaly crest.

CONTENTS

MARITIME SCINTILLATION IN THE EQUATORIAL ZONE

1.0 INTRODUCTION

Equatorial irregularities are known to give rise to amplitude (and phase) scintillation of earth-space radiowaves. This phenomenon, analogous to the twinkling of stars in the optical part of the electromagnetic spectrum, has been the object of research for several decades. Many excellent papers have been published outlining the geomorphology and basic physics underlying this extremely rich and interesting phenomenon. [Aarons, 1978; Crane, 1974; Basu and Kelly, 1979; and recently Basu and Basu, 1981]. NRL and AFGL scientists have contributed to this field through direct (in-situ) measurements of ionospheric plasma characteristics in conjunction with ionospheric plume formation in the equatoral spread F environment [Szuszczewicz et al, 1980; Narcisi and Szuszczewicz, 1981]. In addition, a more fundamental understanding of equatorial scintillation has been derived from computational physics experiments undertaken by the NRL Plasma Physics Group [Ossakow, 1979] and a review of various spread F theories has been published [Ossakow, 1981].

Experimental studies detailing scintillation properties abound in the literature, and many interesting new results have been forthcoming during the current (now receding) solar maximum epoch. Indeed, it was the result of the anticipated increase in scintillation at UHF in the equatorial zone in 1980-81 [Goodman, 1980] which led to the experimental program discussed in this report. Some aspects of L-Band scintillation are also discussed.

The US Naval Research Ship, USNS Hayes (T-AGOR-16), and shown in Figure 1, was scheduled to participate in various oceanographic studies during the first half of calendar 1981, and measurements were to be made throughout the Atlantic basin between Northern temperate latitudes to approximately Antarctica in the Southern hemisphere. This expedition provided a unique opportunity to examine the scintillation phenomenon over a wide range of latitudes under nearly solar maximum conditions. The research capabilities of the Hayes have been discussed by McClinton [1972].

Because of this unique opportunity plans were made to obtain data pertaining to the ionospheric personality in the maritime environment during the 1981 expedition of the Hayes. Accordingly, a Navy UHF Receiver, an AN/SSR-1 (the antenna component is shown in Figure 2 shown installed on the Building 28 roof at NRL), was installed on the Hayes along with a High Dynamics User Equipment (HDUE) GPS receiver. These systems would allow recording of UHF (249 MHz) transmissions of the Navy FLTBCST channel of the Atlantic FLTSATCOM (a synchronous tactical communication satellite located at geosynchronous altitude at a longitude of approximately 22^{o}W) and also the existing complement of NAVSTAR Global Positioning System (GPS) satellites. In view of a number of exigencies associated with delay in acquisition of the necessary GPS HDUE receiver and the necessary system checkout, the GPS data was not available for the whole expedition and is not detailed herein. The UHF data were obtained for the length of the cruise and are the primary subject of this paper. Figure 3 shows the coverage pattern of the Atlantic FLTSATCOM, Figure 4 shows the track of the Hayes, and Figure 5 shows the geographic latitude variation. It is clear that most of the expedition was concentrated in the Southern hemisphere.

Manuscript submitted January 18, 1982.

2.0 EXPERIMENTAL OBSERVATIONS

Upon examination of the scintillation records it was found that nocturnal scintillation was detected much earlier (i.e., at higher geomagnetic and geographic latitudes) than anticipated. The first occurrence of nocturnal scintillation (greater than 30 dB) was evidenced on 7 January 1981, the seventh day of the cruise. This was at 23.33°N, 46.97°W in geographical coordinates and at an approximate geomagnetic latitude of 34°N and a dip latitude of about 24°N. This was not anticipated on the basis of predictions. Evidently solar maximum conditions had enhanced the zone of scintillation occurrence (even though the international sunspot number was "only" 89 on 1-7-81 but its long-term average was higher than this). This is an heuristic deduction but is consistant with current theoretical understanding of the relationship between scintillation and the Appleton anomaly position. More will be said of this later.

Figure 6 is an example of a record of UHF scintillation for Julian Day 61/62 (2-3 March 81) between 2300 GMT and 0600 GMT. Scintillation was deep but not totally continuous (sharp breaks were evidenced). The center of the chart (0200 GMT) is approximately local midnight. It is noteworthy that the AN/SSR-1 receiver, which was tuned to the UHF Fleet Broadcast at about 250 MHz, experienced heavy "fault" activity during the scintillation. This is important for communication purposes.

Analog tape and strip charts were obtained during the course of the expedition and these were returned to NRL for processing.

3.0 DATA ANALYSIS AND PRESENTATION OF RESULTS

Table 1 (two pages) contains the basic data extracted from the preliminary analysis. For each Julian day (at 1200 GMT) are included in the average values of the latitude (LAT), longitude (LON), and ship speed in knots (SPD), the number of quarter-hourly opportunities for scintillation measurement (NBR OBS), the maximum scintillation observed in dB (MAX SCNT), the number of occurrences of scintillation between various ranges, the maximum fade observed (MAX FADE), the magnetic index AFR, the International Sunspot Number (SSN), the geomagnetic dip angle (DIP), the average scintillation (dB), and the average fade level (dB). In the Northern hemisphere scintillation is seen to exhibit a sharp onset (as indicated previously) on 1-7-81 at which time the dip angle (I) was 42°N. This corresponds to a dip latitude of 24°N where $\tan \theta = 1/2 \tan I$. On the return trip scintillation was also observed at a dip angle of I = 61°N (a dip latitude of 42°N) but this may not be related to the typical nocturnal <u>E</u>quatoral <u>S</u>pread <u>F</u> (ESF) phenomenon. In the Southern hemisphere, scintillation was observed as far south as 20°S dip latitude. Although the southern extent of the scintillation was not as great, the magnitude of the scintillation in the Southern hemisphere was greater than that in the Northern hemisphere. The peak average scintillation occurred between -11° and -15° dip latitude (>10dB) in the Southern hemisphere and between +8° and +15.5° (> 7dB) dip latitude in the Northern hemisphere.

During the expedition, equipment outage and other problems were minimal; only on three days were there less than the full 96 one-quarter-hourly intervals monitored for scintillation. Even on these days: 2-19-81, 2-28-81, and 3-1-81, the number of intervals were non-vanishing, being 72, 34, and 93 respectively. This amounted to a total data recovery rate of about 99.4% in terms of the one-quarter-hourly assessments of scintillation. It is

noteworthy that all data loss segments occurred when the ship speed was 0 knots. The significance of this is not as yet known, but it is already not of geophysical importance.

3.1 Geographical Variation

The field data were time-tagged every 15 minutes for the entirety of the 104 days of the Hayes expedition and scaled for maximum fade level and peak-to-peak scintillation over each 15 minute interval. This was done to survey the data prior to the specification of high interest regions for detailed processing, including spectral analysis and correlation of scintillation events with communication system default indications, which were also recorded.

Figure 7 is a calibration curve relating the recorded AGC (Automatic Gain Control) voltage and the input signal level to the SSR-1 receiver. We see that the receiver is roughly linear between 0 and 2 volts. This constituted a dynamic range of about 50 dB.

Figure 8 is a plot of the maximum quarter-hourly UHF peak-to-peak scintillation (dB) observed each day between day 1 and day 104 of the expedition. Figure 9 is the maximum quarter-hourly UHF fade depth (dB). Upon comparison with Figure 5 it is clear that there is a paucity (indeed non-existence) of scintillation when the ship was above 23°N or below 38°S, but there was strong scintillation within these latitudes.

Figures 10 and 11 show the daily variation of the maximum quarter-hourly peak-to-peak scintillation (dB) and fade depth (dB) respectively. The circles represent the amount of scintillation with radii being proportional with the magnitude which ranged between 0 and 40 dB.

Of some interest also, is the geographical distribution of scintillation duration. This is depicted in Figure 12. In this case we have presented in graphical form circles whose radii are proportional to the number of quarter-hourly intervals for which the scintillation exceeded 20 dB. The maximum circle dimension corresponds to roughly 32 intervals (8 hours). It is noteworthy that there were 51 days during the 104 day cruise for which scintillation exceeded 20 dB for at least one (1) quarter-hourly interval. Overall about 200 hours of scintillation ($>$20 dB) was encountered. This corresponds to about 7% of the total observation time including latitude zones where scintillation would not be expected, and daytime periods where scintillation is scarcely observed.

Returning to Figures 10 and 11, we note that within the scintillation zones there are breaks in occurrence of scintillation. In all there were 65 days in which scintillation was observed and 13 days for which scintillation did not occur within the discerned scintillation zone (the Hayes being within the scintillation zone approximately 78 days). Thus, nocturnal scintillation within the zone occurred on 84% of the "opportunities". The reason for these periods of no scintillation is not known.

3.2 Organization of Data by Geomagnetic Dip Angle

Figure 13 shows the daily variation of magnetic dip angle during the Hayes expedition. Figures 14 and 15 are plots of the maximum daily quarter-hourly values of peak-to-peak scintillation (dB) and scintillation

fade depth (dB) respectively. Although the number of data points is sparse in the Northern hemisphere, certain tendencies are clear. First, there is a sharp cut-off of scintillation when the dip angle (I) of the geomagnetic field exceeds 40° in absolute value. Secondly, there is a tendency for the scintillation to be somewhat diminished at the dip equator itself. This would have been predicted based upon past studies.

Figure 16 depicts the number of strong ($\geq$20dB) scintillation intervals for each day organized in terms of magnetic dip angle. Aside from the manifestations of the $|I| > 40^{\circ}$ cut-off, there is no obvious pattern. The greater scatter in the Southern hemisphere may simply be the result of more opportunities in the region. It is noted, however, that for a dip latitude of about -13.6° (-26° dip angle), there exists the most statistically significant number of high ($>$20dB) scintillation occurrences. Between a dip latitude of about -9° and -16°, there were no observation days for which at least 5 hours of strong ($>$20dB) scintillation did not occur.

Another perspective can be obtained by averaging the data. Figures 17 and 18 are dip-angle-averages of the maximum UHF scintillation (peak-to-peak) and scintillation depth respectively. Although the patterns are not strictly symmetrical about the dip equator (dip angle = 0) there is a degree of symmetry. The peak-to-valley ratio is 10 dB. Also shown are the number of data points entered into each average per 5 degree latitude "cell". Clearly, the Southern hemisphere is covered more fully.

Figure 19 is the average plot corresponding to Figure 16. Most of the data were obtained for a dip angle less than or equal to -10°. At a magnetic dip angle of about -26°, the average number of scintillation observations (one-quarter-hourly intervals $>$20dB) was about 25 and this corresponds to an average duration of about 6 hours. As indicated above, this dip angle maximum corresponds to a dip latitude of -13.6°.

Figures 20-23 are plots of the scintillation initiation start times (referenced to local midnight) for scintillation $>$30dB, $>$20dB, $>$10dB, and $>$0 dB respectively. Larger "lead" times mean that scintillation occurred "earlier" in the evening. At high latitudes in the South American sector, the scintillation started later in the evening than at intermediate latitudes (say near 16° dip latitude or 30° dip angle). In the more nearly equatorial zone (say -5° dip latitude) the scintillation onset began to approach midnight again. The overall pattern appears to be represented by less rapid onset at the edge of the scintillation zone ($\pm 40^{\circ}$ dip angle or $\pm 23^{\circ}$ dip latitude), a more rapid onset at intermediate equatorial latitudes, and a slight dip near the geomagnetic equator (but favoring the South American zone).

3.3 Diurnal Variation of Scintillation

There is also a wide variation in the behavior of scintillation with respect to the diurnal cycle. Figure 24 shows a more typical example of the quarter-hourly fading range with respect to the mean signal level. Figure 25 is the magnitude of the fading range (peak-to-peak in dB). Figure 26 shows that scintillation occurrence during the night may be quite erratic.

3.4 Distribution of Scintillation Depth

Two types of distributions typically occur, but again there are wide variations. The more distinctive types are shown in Figures 27 and 28.

Figure 27 shows essentially an "on-off" type of scintillation; whereas Figure 28 shows that two equally probable distributions sometimes occur on a given day, one corresponding to somewhat moderate fading amplitude and the second corresponding to strong scintillation. There was virtually never a situation for which only moderate fading was observed on any given day.

4.0 DISCUSSION

4.1 Selected Comments on Equatorial Aeronomy

In order to explain the geographical pattern of UHF scintillation observed during the USNS Hayes expedition, in particular its broadened latitudinal extent, it is necessary to briefly comment on the current state of knowledge of "Equatorial Spread-F (ESF)" from a geomorphological and physical point of view.

Basu and Basu [1981] have recently reviewed equatorial scintillations, especially for GHz frequencies and reviews of Equatorial Spread F [Kelley and McClure, 1981] and various spread F theories have been published [Ossakow, 1981]. The reader is also directed to the proceedings of the Sixth International Symposium on Equatorial Aeronomy [Matsushita et al, 1981] and the Proceedings of the NRL/AFGL sponsored Ionospheric Effects (IES '81) Symposium [Goodman, Clarke, and Aarons, 1981]. Additional information of interest has been disclosed in the recent URSI General Assembly booklet of abstracts [URSI General Assembly/Washington, DC, 1981].

It is currently believed that equatorial scintillation is peaked near the crests of the equatorial (Appleton) "Anomaly" and this is particularly intense in the American zone. Phenomenologically we find that when noontime values of the ionospheric electron densities are observed (specifically F2 maximum densities), two peaks are found situated on either side of the geomagnetic equator [Maeda et al, 1942; Appleton 1946; Maeda, 1955]. The position and strength of this anomalous behavior exhibits a strong diurnal and longitudinal variation and there are seasonal variations as well. The anomaly is thought to be formed by the combined effects of $\vec{E}\times\vec{B}$ drift and ambipolar diffusion. Following sunrise, dynamo action in the E region produces an Eastward-directed electric field and this electric field operates on the F region plasma producing an upward drift (by the right hand thumb rule). The velocity of this drift is proportional to the strength of the electric field ($\vec{V} = \vec{E}\times\vec{B}/B^2$) where E is in volts/m, B is in Tesla, and V is in m/sec. Another process causes this plasma to diffuse downward along magnetic field lines (gravitational force and the pressure gradient force). Diffusion is known to be a major factor in controlling the shape and behavior of the upper F region. This diffusion process was initially invoked to explain the positioning of the F2 layer peak. It occurs only along magnetic field lines and depends upon electron density and temperature gradients as well as the plasma scale height. Diffusive equilibrium is disrupted if the scale height of the topside F region changes rapidly. This would occur over the equator as the result of an $\vec{E}\times\vec{B}$ source of bottomside plasma. In any case, the net effect is that equatorial ionization (plasma) is transported to both the north and south of the equator producing a relative minimum at the equator and peaks surrounding the equator [Anderson, 1973]. The accepted mechanism for describing the Appleton or equatorial anomaly - sometimes called the "fountain effect" is due to Martyn [1947]. The Appleton anomaly actually begins during the daytime (around 1100 LMT) and progresses poleward to larger dip (inclination) angles. The anomaly reaches its maximum development at about 2000 hours LMT with the crest nearer to the geographic equator being the most

daily variations in the geomagnetic field. The reader is reminded of the basic principles of dynamo theory which are listed below:

- (i) Tidal forces introduced by the sun and the moon (24 hour periodicities).
- (ii) Tidal forces produce standing waves which cause large horizontal air motion.
- (iii) Air motion across the earth's geomagnetic field gives rise to (induces) EMF forces which drive currents in the E region because of the large conductivity there.
- (iv) Polarization charges are introduced which modify the flow of current; this is caused by spatial variations in electrical conductivity.
- (v) The polarization charges generate electrostatic fields which cause electrodynamic drifts.

In addition to the E-region dynamo, which is obviously central in the production of the Appleton anomaly, there also exists an F-region dynamo driven by the global thermospheric wired patterns [Rishbeth, 1981].

As indicated above, the post-sunset behavior of the vertical F region drift can most likely not be accounted for by the assumption of tidal-E region fields alone [Rishbeth, 1981]. (This argues for increased importance of the F-region dynamo action). The F-region dynamo fields, also driven by winds in the F region, are not important in the daytime since they are short circuited by the large E region conductivity. However, at night, and especially at sunset when the E region (and its conductivity) disappears, a substantial F region polarization field develops. The F region dynamo most likely is a candidate to explain the "pre-reversal" enhancement in vertical plasma drift at 2000 LMT. Furthermore, it has been shown by Heelis et al [1974] that during the evening and pre-midnight hours there exists a shear in the East-West plasma drift velocity. Near the F2 peak and above the flow is to the East, below the F2 peak the flow is Westward. The topside Eastward motion is caused by the polarization field in the F-region which however, operates inefficiently in the E-F valley region below the F2 peak. The bottomside motion (evening zonal plasma motion) is westward being driven by E region Westward-directed E fields generated to the North and South of the dip equator and coupled to the valley region along magnetic field lines. The F region polarization field therefore builds up at night and this "open circuit" condition drives plasma rapidly to the East. The polarization field reaches a value of UB where U is the neutral air speed [Rishbeth, 1981]. For B = 30 UT and U = 200 m/sec, the polarization E field = 6 m V/m. This field may drive the equatorial thermospheric gas at greater than the earth's rotation velocity - "super rotation" - by the process of ion-neutral drag. The "normal" F region vertical drift - driven by the E region dynamo - is downward at night and upward during the day. However the polarization field in the F region (which drives the super rotation at night) also may have east-west components especially at sunrise and sunset. This yields vertical drift. The sunrise effect is small because of low relative F region density.

The $\vec{E}x\vec{B}$ drift caused by the F region dynamo and preferential bottomside recombination following sunset causes a net upward movement of middle and upper F region plasma and a steepening of the bottomside gradient of electron density. The tendency to development of irregularities in the F region at night is not prevented since there is no E region conductivity. According to Ossakow [1981] the steepened bottomside is conducive for growth of plasma

density fluctuations by collisional Rayleigh-Taylor, $\vec{E}\times\vec{B}$ gradient-drift, or other fluid-type gradient instabilities. The process is now one in which polarization $\vec{E}\times\vec{B}$ fields will drive the plasma density depletions (non-linearly) vertically through the ionosphere to the topside. Their presence on the topside produces spread F on ionograms. Equatorial spread F (ESF) constitutes a range of irregularities producing scintillation as well. According to the "plume" theory, the plasma bubbles become steepened on their topsides, bifurcation occurs, and the process cascades.

The maximum altitude reached by the plasma bubbles is of considerable importance especially since the Hayes-related scintillation occurred at such great latitudes suggesting that the ESF was mapped (along field lines) from exceedingly high altitudes. Using data obtained from the Allouette 2 and ISIS I topside sounders, Benson [1981] has remotely detected the maximum altitude of equatorial ionospheric plasma bubbles. Dyson and Benson [1978] have previously examined the field-aligned nature of this class of irregularities. The observations by Benson are of ducted HF sounder signals which are guided along geomagnetic field lines (actually being guided by the irregularities in refractive index or electron density which are aligned with the B field). He finds that the maximum bubble altitudes may exceed 2000 km but <u>this is principally in the American sector</u>. This fact is consistent with the suggestions of plume altitude from the Hayes observations.

4.2 Soviet Maritime Observations

Other collateral information is available from Soviet scientists who have taken data aboard moving platforms [Ben'kova et al, 1978; Vasil'yev et al, 1979]. These investigations utilized vertical incidence (bottomside sounders) aboard the R/V Akademic Kurchatov and Zarya during the period 1959-1977. In the first paper, the soviet workers characterized the F-region irregularity zone as consisting of two "additional stratifications" centered about the geomagnetic equator. These stratifications are typically observable during daytime however and unless the effects are limited by the observational technique are not directly relatable to nocturnal ESF phenomena. They are likely just manifestations of the well-known Appleton anomaly. In their second paper a more concerted effort was directed toward investigation of spread F. Even so, only daytime spread F was considered (between 0700 and 1900 LMT). The main point to be emphasized from these studies is that the probability of "spread F" increases with solar activity as does the latitude zone of the disturbance.

4.3 L-Band Scintillation Data

The strong intensity of the UHF scintillation observed during the Hayes expedition precludes specification of an unambiguous diurnal and geographical distribution of equatorial irregularities responsible for the effect. However, the expanded latitudinal distribution is quite noteworthy. The L-band signals from the GPS satellite obtained during a portion of the expedition may partially assist in the elucidation of the irregularity formations. In particular, since the Total Electron Content (TEC) of the ionosphere may be extracted from the GPS data, it may be possible to correlate depletion zones with the observed scintillation [Klobuchar, 1978; Yeh et al, 1979]. Of primary interest is the location of the crests of the Appleton anomaly in the Northern and Souther hemispheres. Since the scintillation amplitude is likely to be the product of ambient density and irregularity amplitude, scintillation might be expected to be larger near the crest than

within or on the poleward sides. However, this is an heuristic deduction and not a rigorous argument. Nevertheless, it has been recently shown that GHz scintillation is abnormally pronounced near Ascension Island, not far to the east of the near-equatorial Hayes measurements [Aarons et al, 1981]. This intense scintillation is not replicated at similar geomagnetic latitudes away from the Atlantic basin.

Figure 29 due to Klobuchar [1981] shows the L-band scintillation which was observed at Ascension Island during January - February 1981. Analysis of the NRL Hayes GPS data is now being pursued with the highest priority.

4.4 Comparison with the SRI Model

According to the model of scintillation developed by Fremouw and Rino [1978], the scintillation index S_4 exhibits twin peaks, the midpoint of which lies on the geomagnetic equator. The diurnal pattern of this feature is illustrated in the sequence of Figures 30-32. (The plots are contours of scintillation index at fixed Universal Times for the case of 250 MHz transmissions from FLTSATCOM located at 0^o latitude and 23^oW. The shaded region is the zone for which S_4 is greater than or equal to unity according to the model. (Solar maximum conditions are assumed with the 10.7 cm solar flux index = 200, and $k_p = 6$). The model suggests that the $S_4 = 1$ condition is a relatively narrow bifurcated band of latitudes. On the other hand, the Hayes data indicates that the $S_4 = 1$ condition is significantly larger than this and perhaps encompassing virtually all of the South American latitude region. This discrepancy is now being scrutinized very carefully. It is remarked that in the American Sector the magnetic equator lies 12^oS of the geographic equator at 85^oW geographic latitude. Furthermore, the geomagnetic field strength is relatively lower in the American Sector than other zones, say the Asian Sector. These distinguishing features in the American zone make the results obtained during the Hayes expedition quite interesting.

4.5 Solar and Magnetic Activity

For completeness, a comment on solar and magnetic activity is in order. Figures 33-35 show the International sunspot number (R_I), the 10.7 cm flux index, and the Fredericksburg "A" index respectively. It is clear that the solar activity is quite large during the observation period. However, the magnetic activity levels were not particularly large except on isolated occasions; its impact may have been minor. It has been suggested that whereas solar activity has a positive effect on equatorial scintillation levels, the impact of magnetic activity control is to diminish the S_4 index. If this is the case, we have the situation for which values of both of the external "driving functions - R_I and A" serve to enhance scintillation around the equatorial zone.

5.0 Concluding Remarks and Recommendations

The scintillation data obtained during the 1981 expedition of the USNS Hayes exhibited all of the usual features one would have expected; strong saturated scintillation only at nighttime with rapid and steep onset near the equatorial zone, somewhat irregular diurnal behavior suggesting pathiness, scintillation which is stronger in the pre-midnight period than the post-midnight period, and stronger scintillation surrounding the dip equator than at the equator itself.

However there were some interesting features observed which were not fully anticipated. First, it was found that scintillation occurred at much greater dip latitudes than predicted or observed previously. This suggests that the seat of the irregularities is influenced by a combination of forces which (a) causes the equatorial fountain to operate more efficiently and (b) which drives the equatorial plumes to higher altitudes than might be expected. The maximum dip latitude at which scintillation was observed was about $\pm 23^{\circ}$. The field lines passing through these latitudes pass over the dip equator at an altitude of approximately 2200 km. This is certainly consistent with the recent findings of Benson [1981] based upon Alouette and ISIS I data. However, as indicated in the report, the effectiveness of irregularity mapping to higher latitudes is crucially dependent upon the position of the Appleton anomaly. Evidently the anomaly itself is expanded during solar maximum conditions. It is unlikely that the predicted anomaly crest position of $\pm 16^{\circ}$ (in dip latitude) could sustain strong scintillation at $\pm 23^{\circ}$ (dip latitude).

To recapitulate, we think that the larger values of solar activity observed during the 1981 Hayes observations were conducive for the development of enhanced $\vec{E}\times\vec{B}$ forces (via the E-region dynamo) which served to raise the F2 plasma altitude and resulted in a greater poleward expansion of the Appleton anomaly crests. At the same time the enhanced phase drifts steepened the bottomside gradient of plasma density more markedly over the equator yielding a situation favoring the development of plasma fluctuations. The large plasma depletions, thus formed, were driven upward by the $\vec{E}\times\vec{B}$ polarization fields. These depletions, or plumes, are thought to cascade into an hierarachy of irregularities as they ascend to the topside F region. Because of their greater probability of formation, given the conditions cited, and the greater initial velocity during solar maximum conditions, there exists a greater likelihood that scintillation-producing irregularities will be mapped (along field lines) to the geomagnetically-distended latitudes traversed by the USNS Hayes. However this is not totally sufficient. Because the anomaly crests were also distended in latitude (i.e., poleward) during the observation period, the radiowave scintillation zone was also expanded. This would explain the results.

The current work is based upon an ad-hoc opportunity provided by an oceanographic expedition of the USNS Hayes. However, the experiment was clearly non-optimum from the point of view of separating out seasonal from other factors such as solar and magnetic activity. Also the Hayes cruise favored the southern hemisphere and the data base was accordingly limited in the Northern zone of the Appleton anomaly. Given the sporadic nature of scintillation, general conclusions based upon the current data sets must be reached with caution as a result of these factors.

Were opportunities to arise again to obtain maritime scintillation data, it would be advisable to interact fully in the development of the operations plan to achieve a balanced set of latitudes at which data is obtained. From a scientific point of view it is recommended that future scintillation data be obtained in concert with bottomside ionosonde data obtained from a sounder located on the ship. All future operations should also include GPS data collection as well.

Immediate future plans include processing the L-band GPS data obtained during the Jan-April expedition of the USNS Hayes. Hopefully more insight will be gained by incorporation of these data sets. This specifically refers

to the TEC variations which may be obtained unequivocally. Position of the anomaly and its relationship to UHF scintillation may be obtained as a result.

6.0 ACKNOWLEDGMENTS

The authors would like to acknowledge the assistance of Mr. C. Myers and Mr. J. Stewart, both of NRL for their efforts in software development. Also we would like to thank Messers L. Harnish of NRL and T. Priddy, L. Quinn, V.B. Richards, S. Buisson, and T. Wilson of Bendix corporation for their contribution to both the data collection and processing. Finally a tremendous debt of gratitude is owed to Mr. H. Flemming of NRL who allowed us the opportunity to take part in the USNS Hayes expedition.

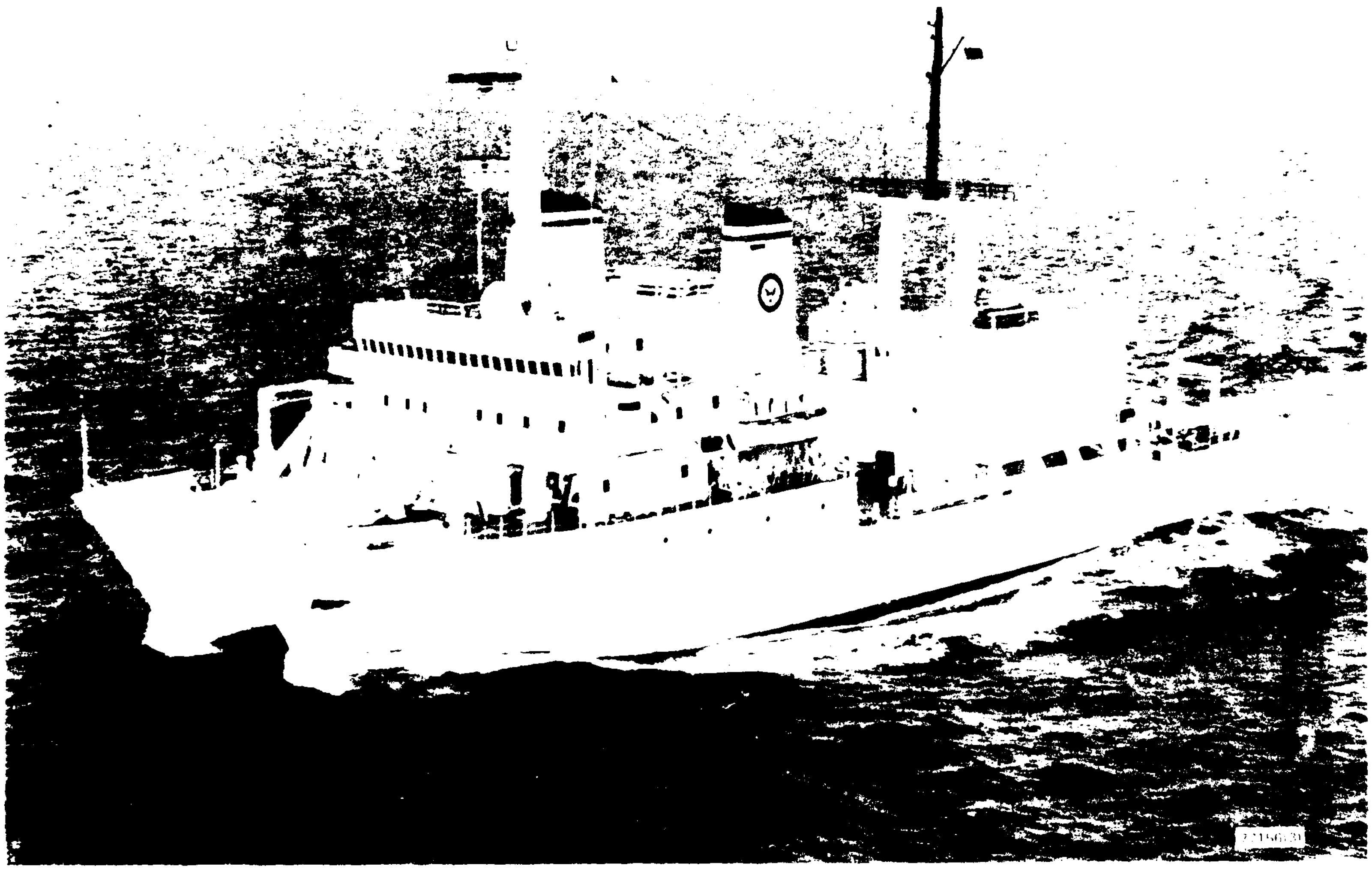

Fig. 1 - USNS Hayes (T-AGOR-16)

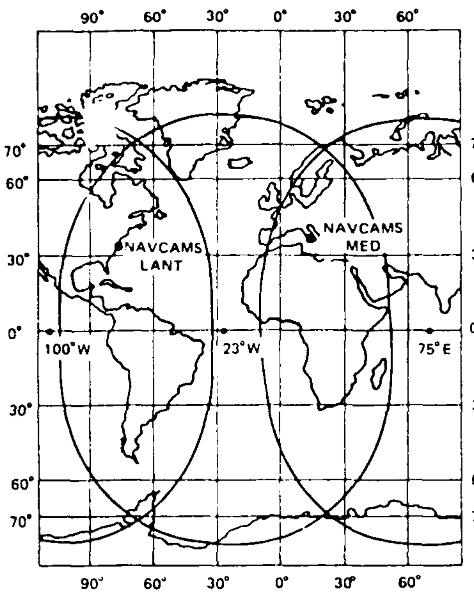

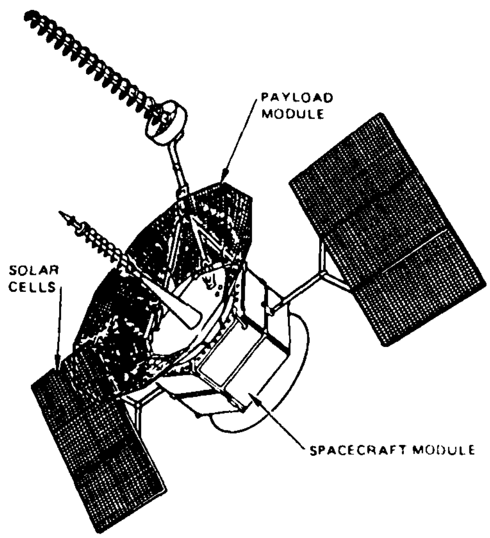

FLTSATCOM Satellite

Fig. 3 - Coverage pattern of the various FLEETSATCOM satellites. The Atlantic FLTSATCOM is located at approximately 23°W longitude. The satellite is also shown on the right of the Figure.

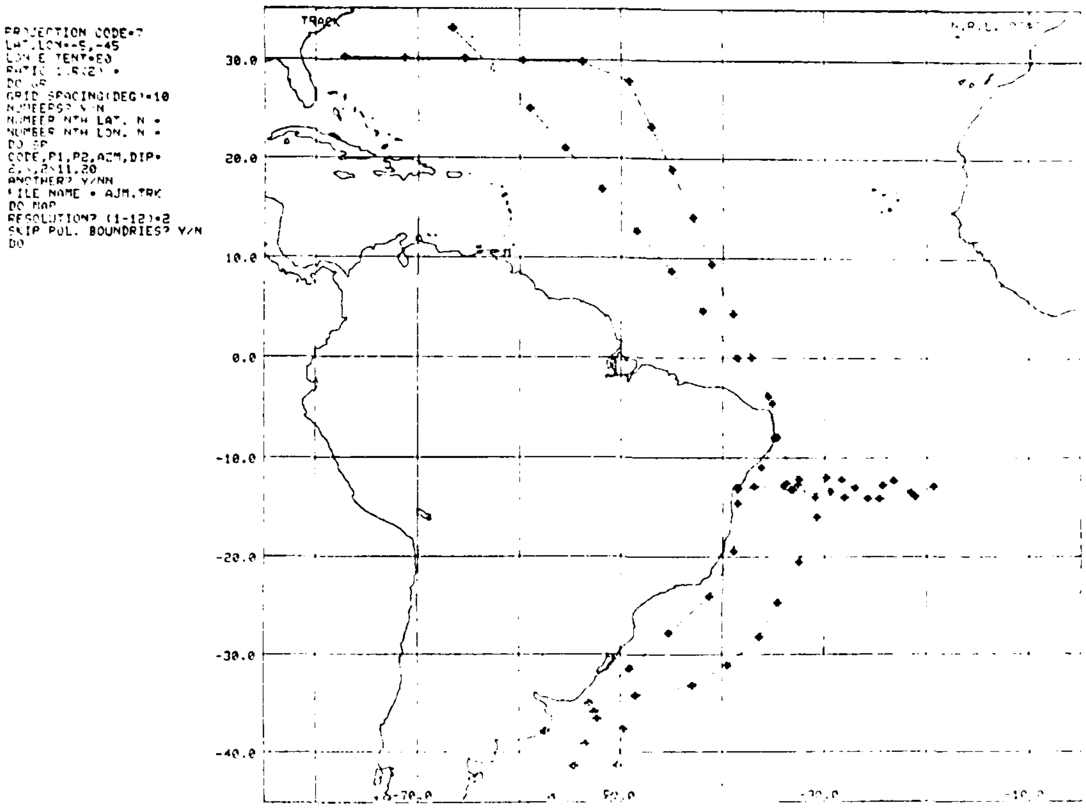

Fig. 4 - Computer representation of the track of the USNS Hayes between 1 Jan and 15 April 1981

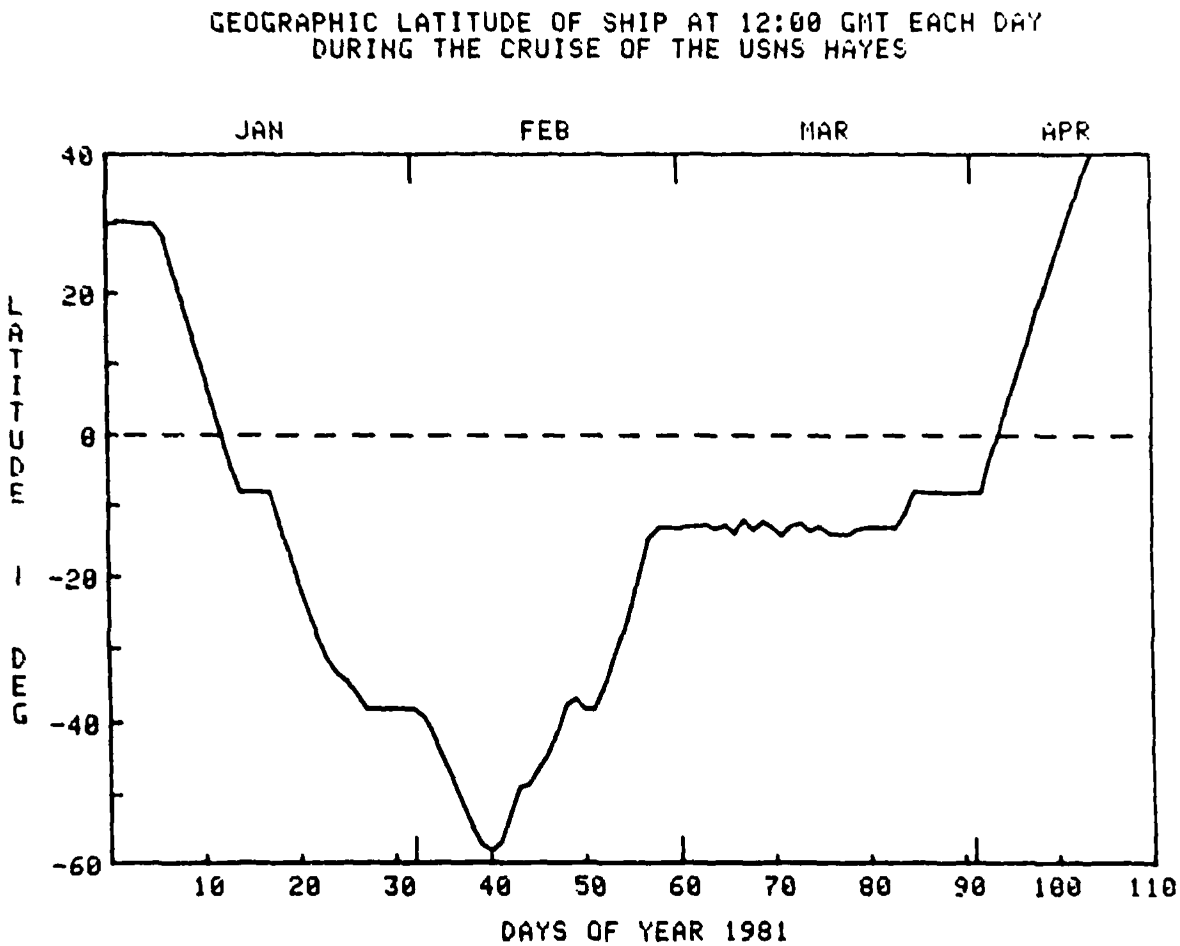

Fig. 5 - Geographical latitude variation of ship position

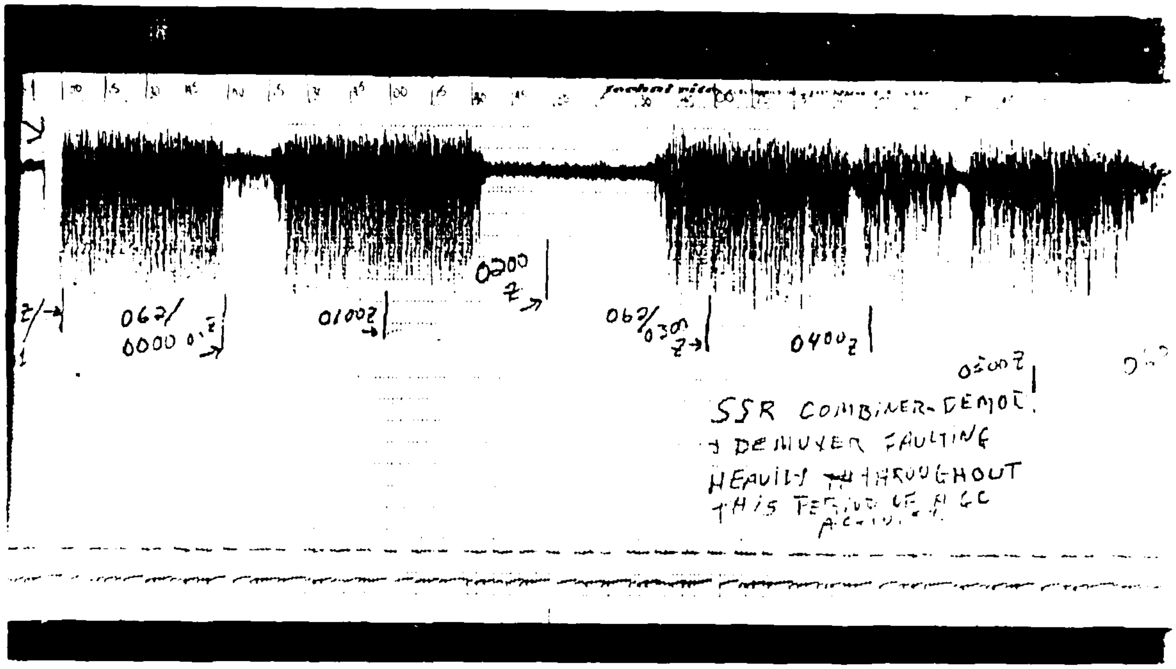

Fig. 6 - Record of UHF scintillation on Julian Day 61/62. The maximum fading experienced in this case is about 35 dB.

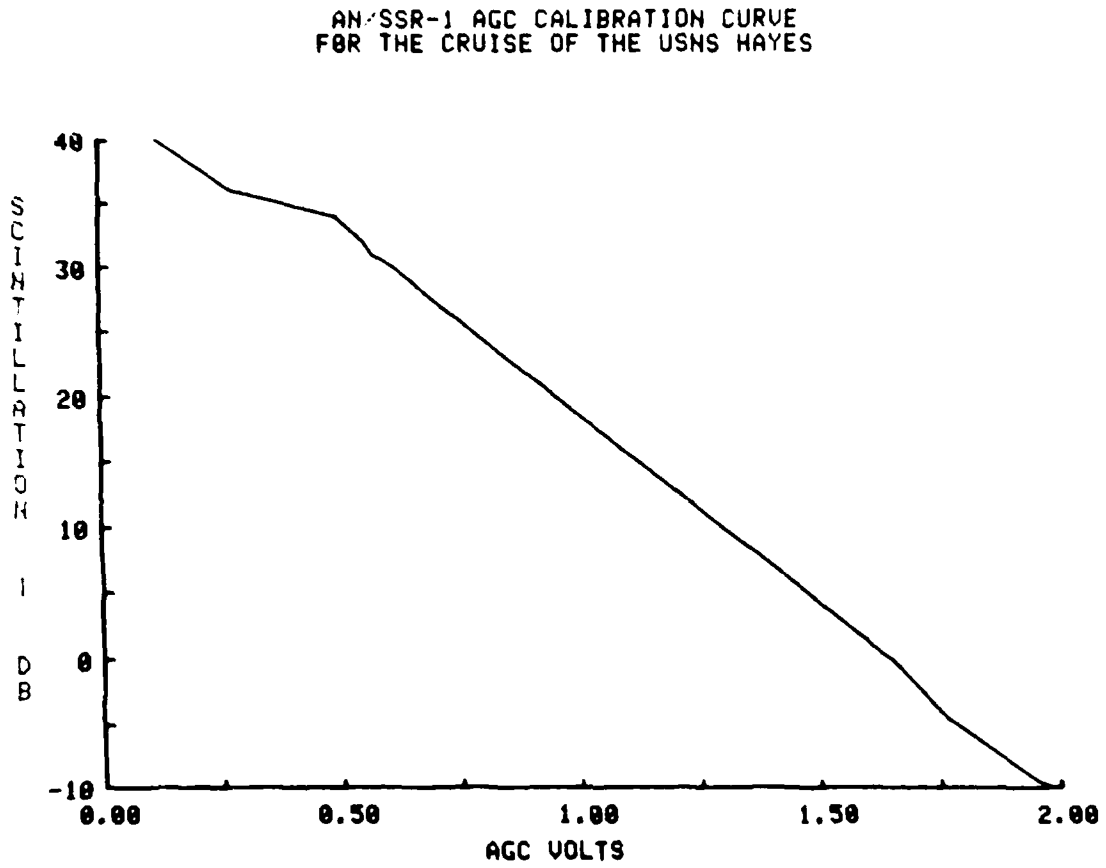

Fig. 7 - AN/SSR-1 calibration curve. A dynamic range of about 50 dB is indicated.

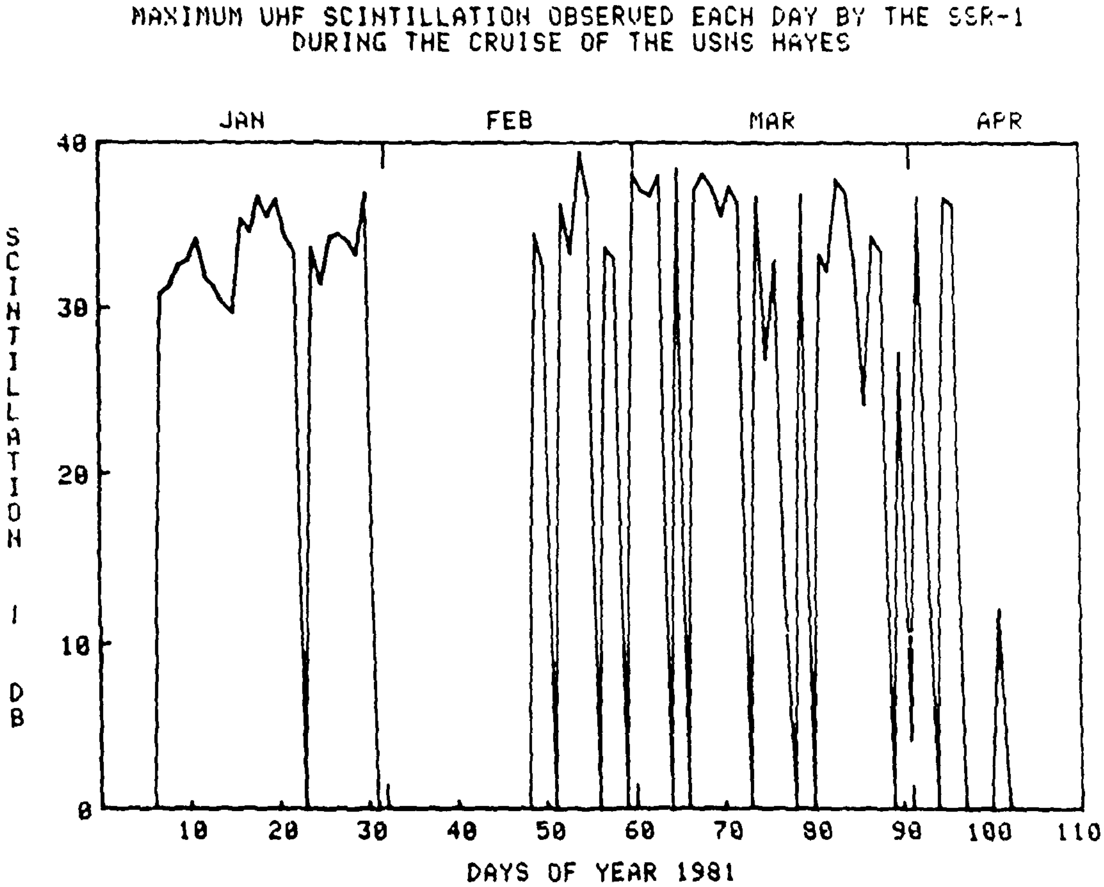

Fig. 8 - Maximum quarter-hourly UHF peak-to-peak scintillation (dB)

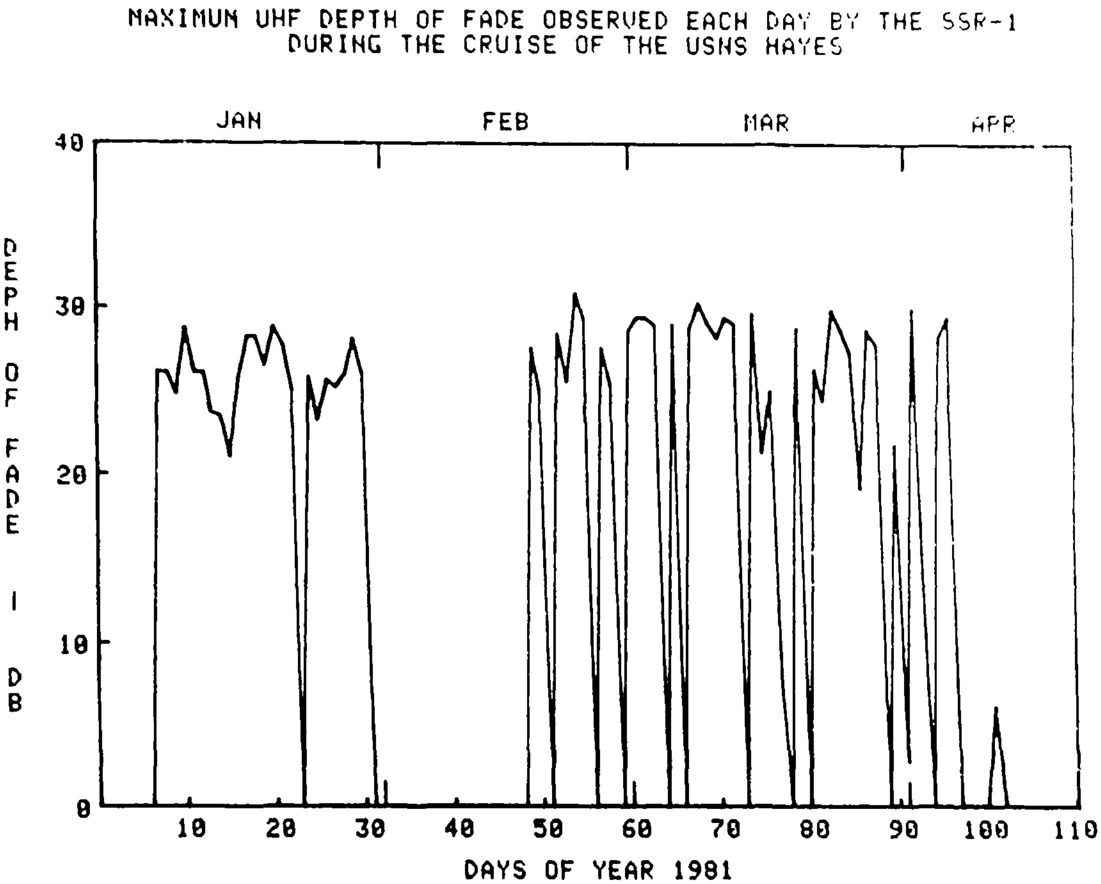

Fig. 9 - Maximum quarter-hourly UHF fading depth (dB)

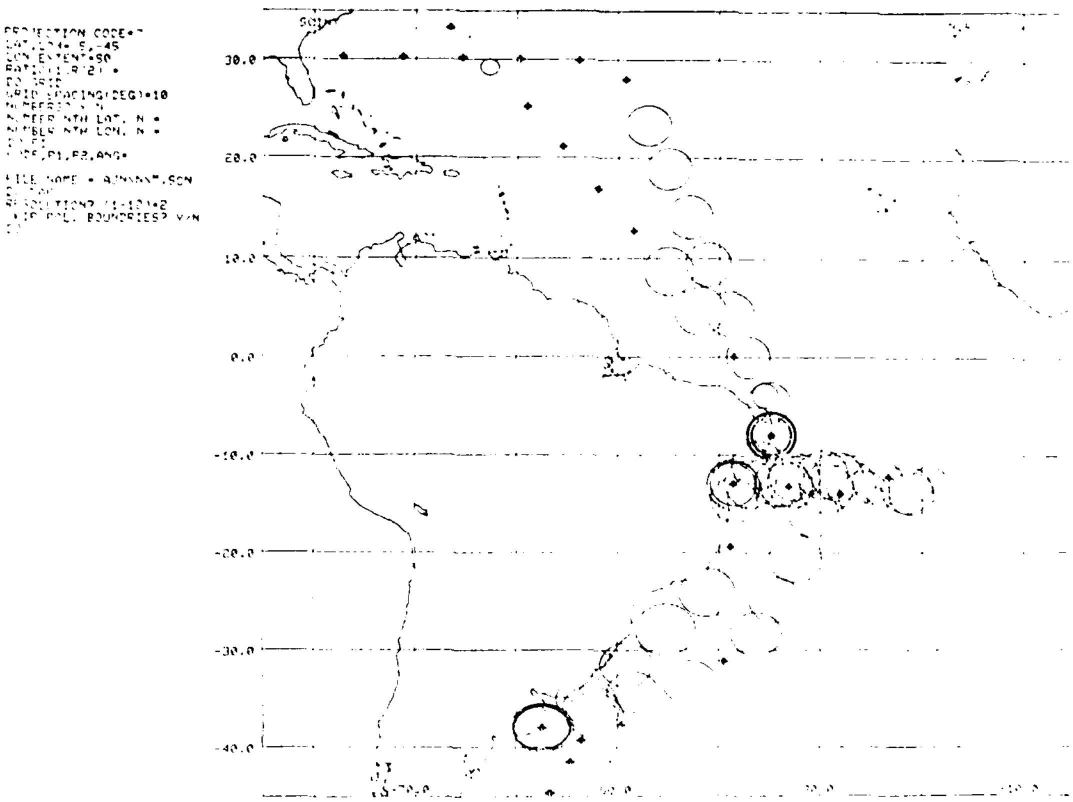

Fig. 10 - Representation of the daily variation of the maximum quarter-hourly peak-to-peak scintillation (dB). The circle size is proportioned to the magnitude of the scintillation and should not be confused with an "area" of scintillation. The actual data points are at the center of the circles.

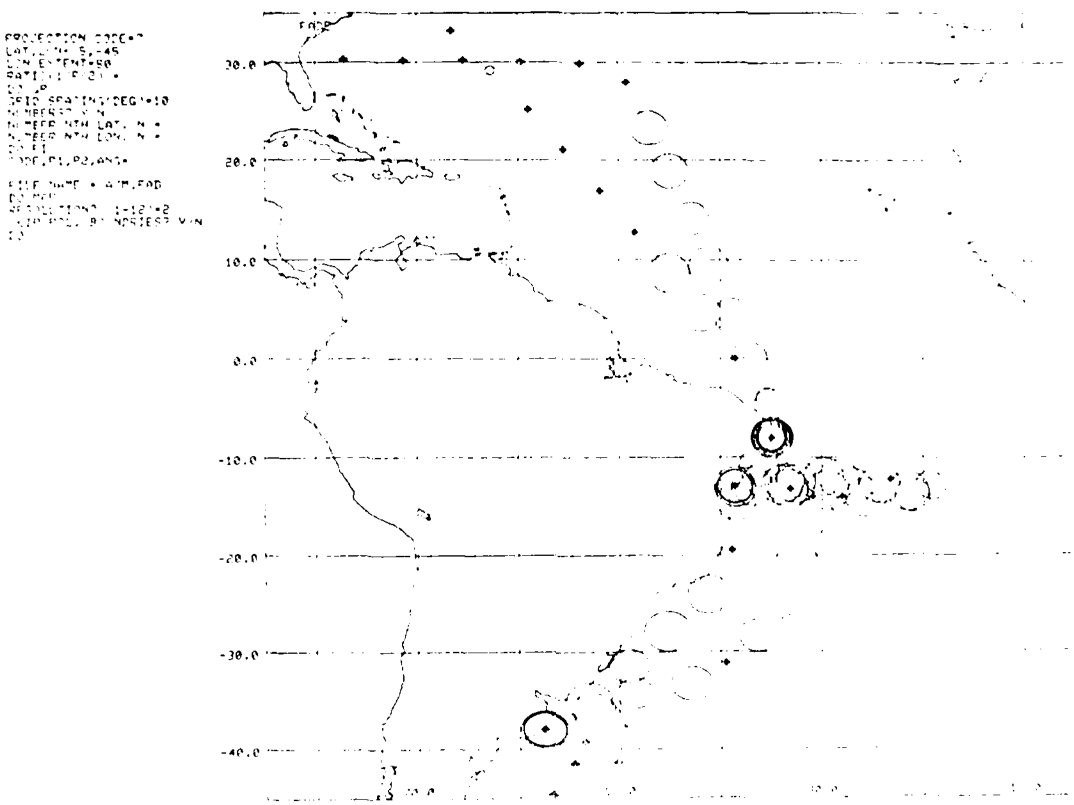

Fig. 11 - Same as for Figure 10, but fade depth (dB) is considered

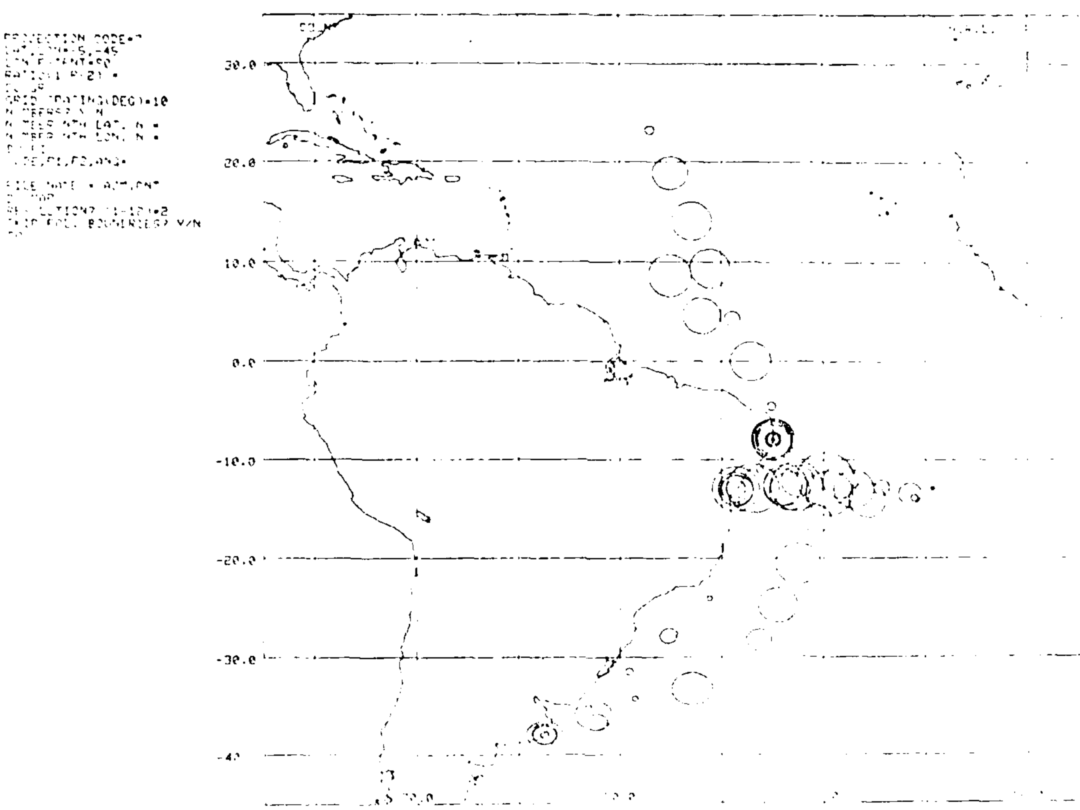

Fig. 12 - Same as for Figures 10 and 11 except the number of quarter-hourly intervals for which the scintillation exceeded 20 dB per day is presented

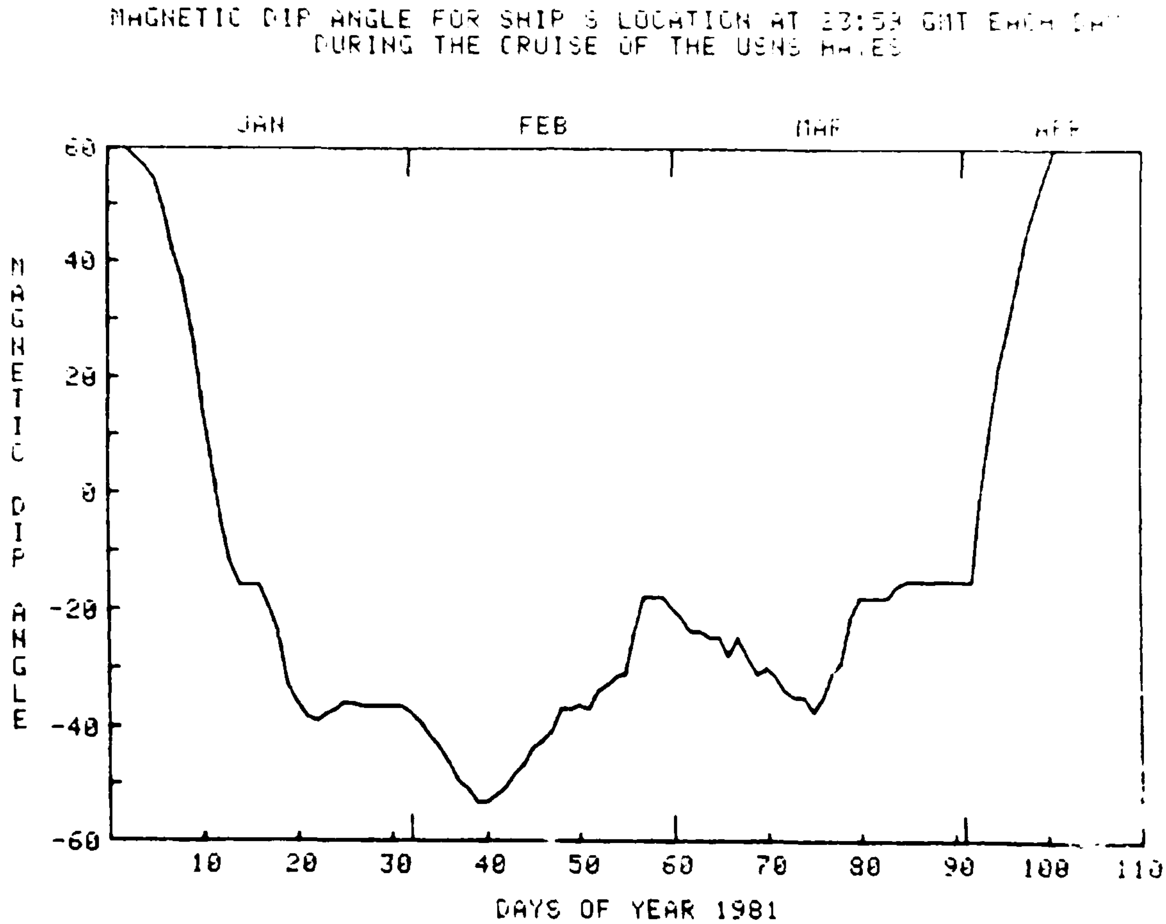

Fig. 13 - Daily variation of the geomagnetic dip angle during the Hayes expedition

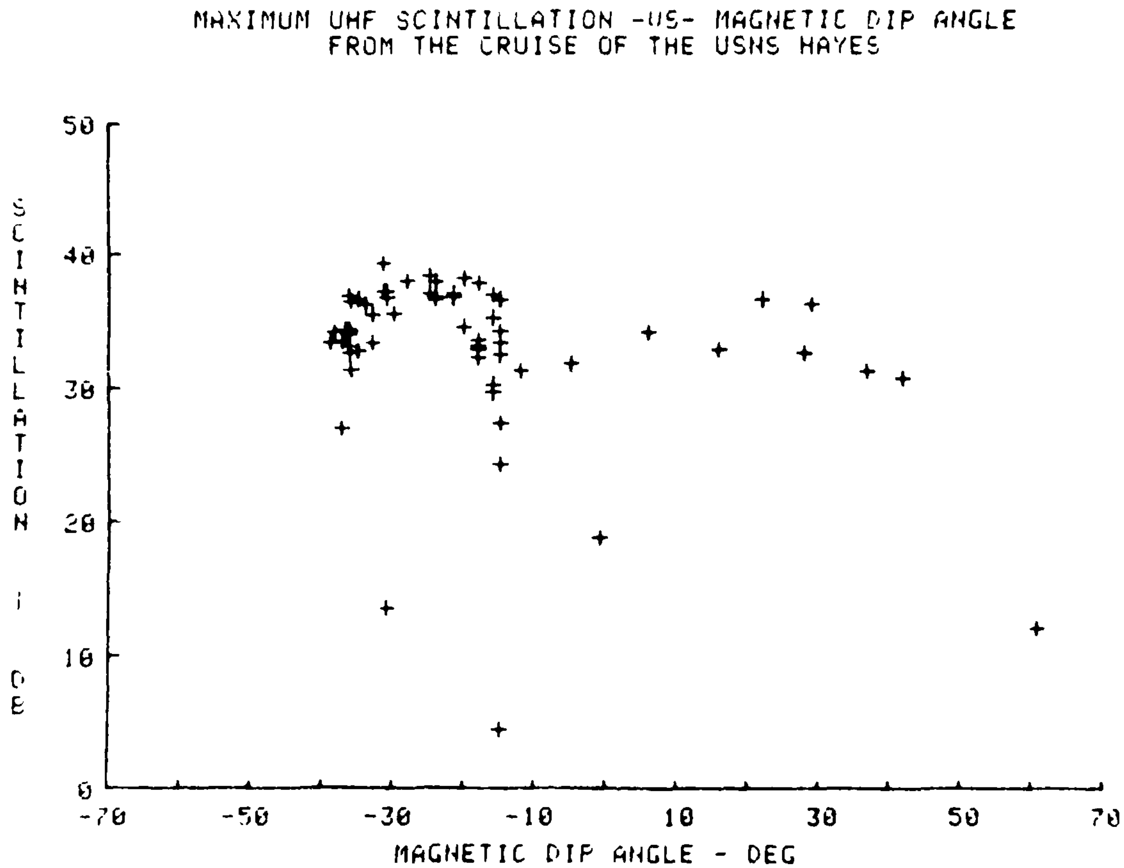

Fig. 14 - Maximum daily quarter-hourly values of peak-to-peak scintillation (dB) versus magnetic dip (I) angle.

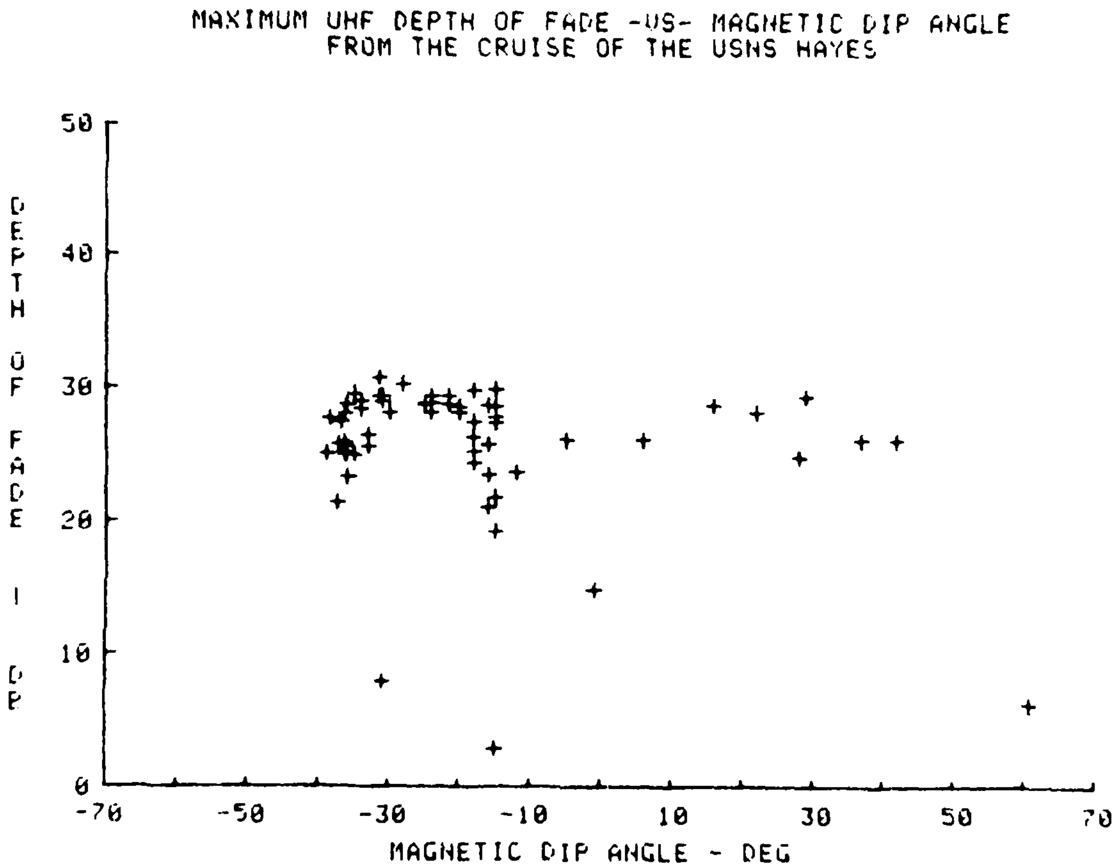

Fig. 15 - Same as Figure 13, except fade depth (dB) is considered

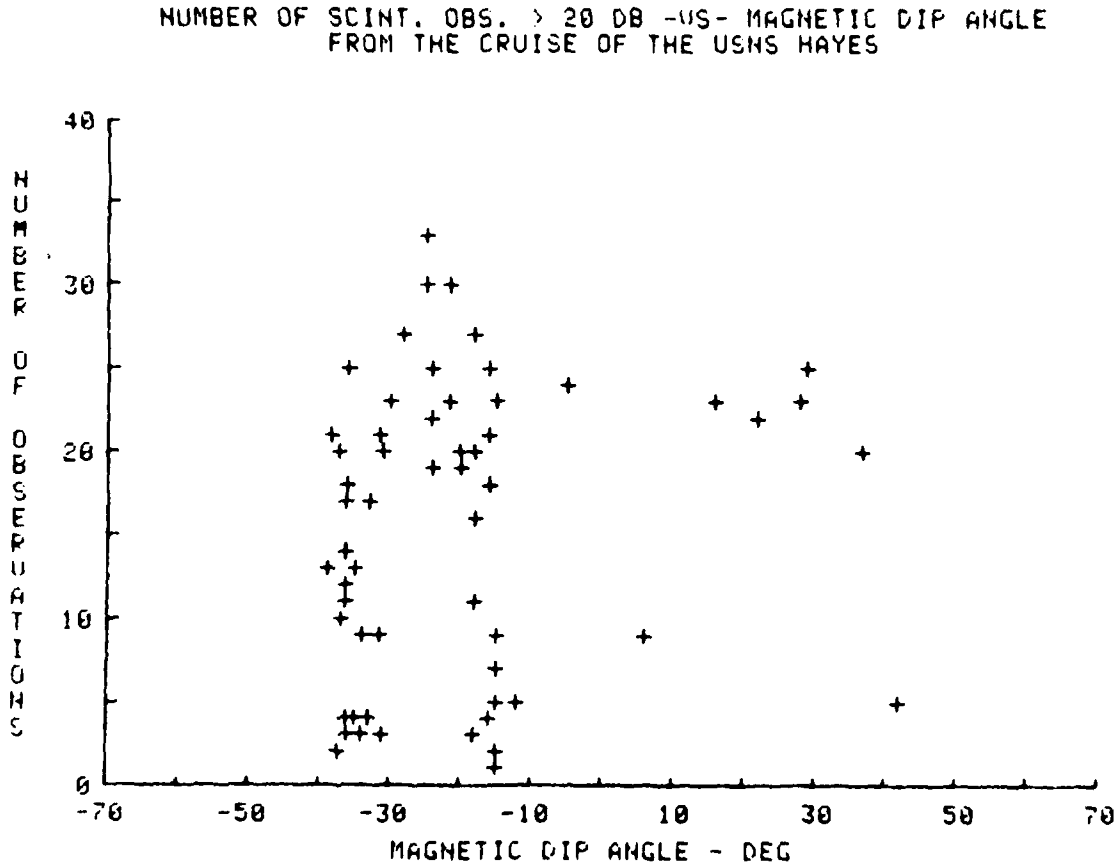

Fig. 16 - Same as Figures 13 and 14, except the number of occurrences for which the maximum quarter-hourly peak-to-peak scintillation exceeded 20 dB is considered.

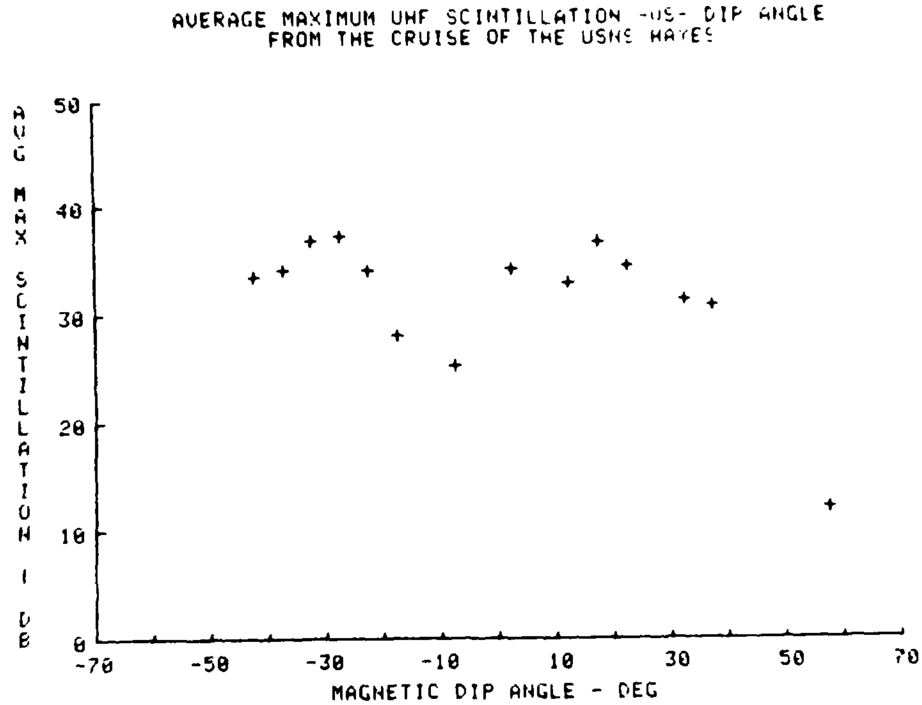

(A)

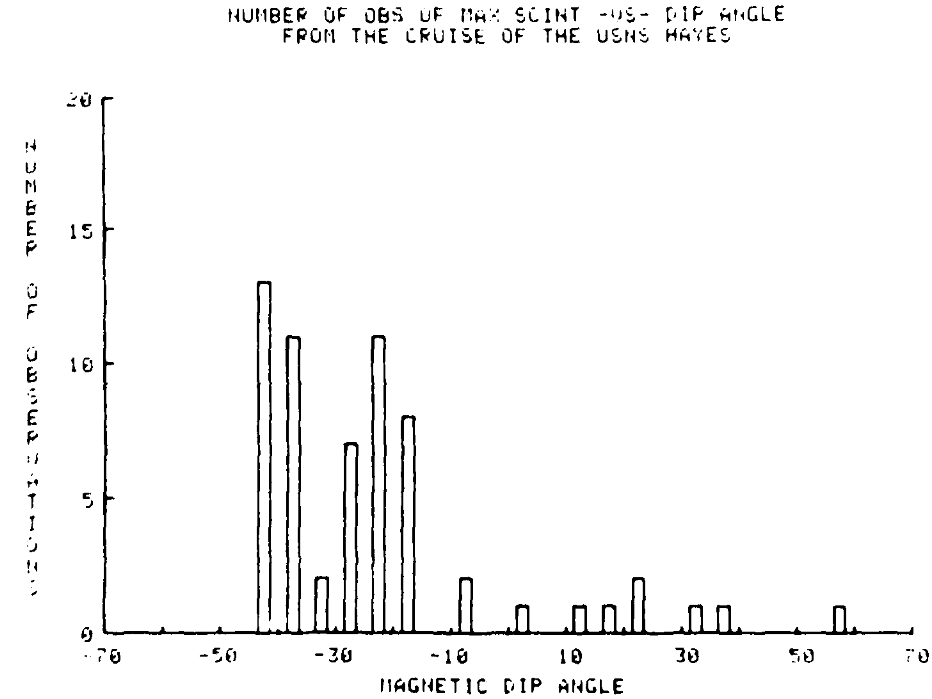

(B)

Fig. 17 - (A) Average maximum UHF scintillation vs. dip angle.
(B) Number of occurrences used in average.

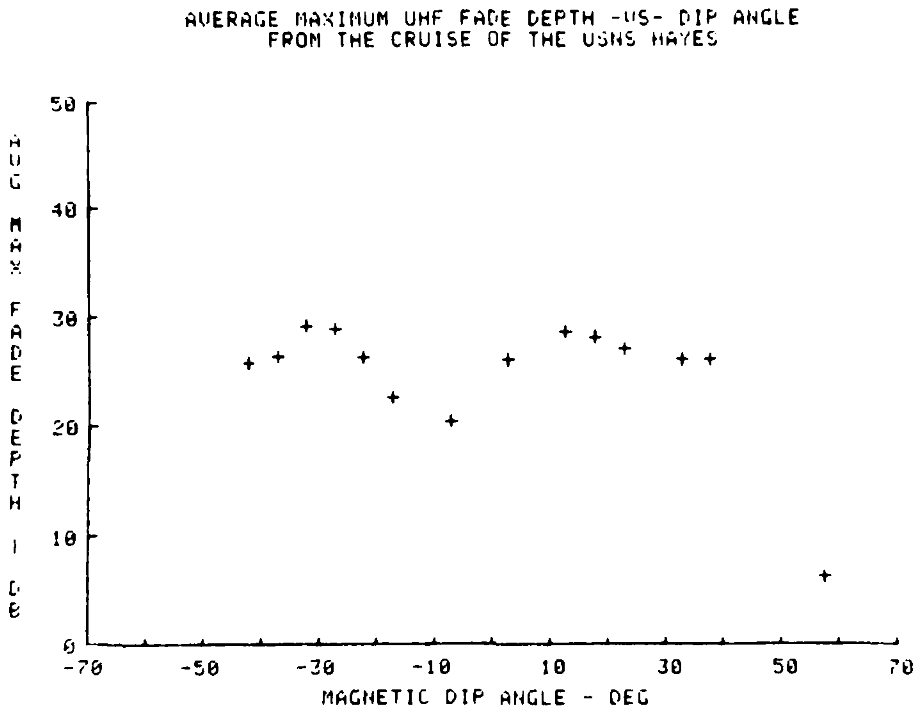

(A)

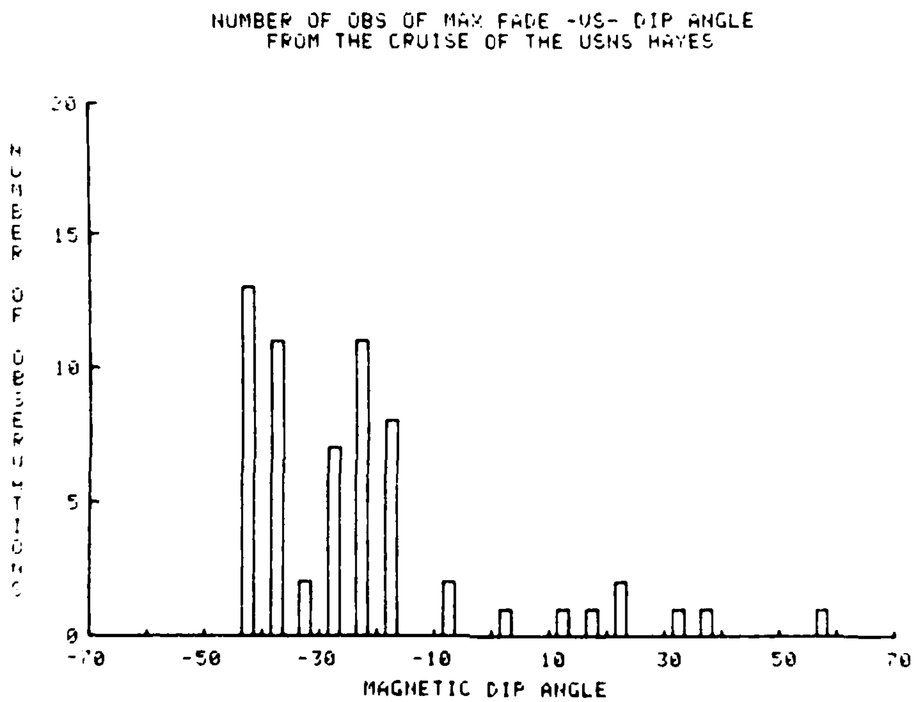

(B)

Fig. 18 - (A) Average maximum UHF signal fade depth vs. dip angle.
(B) Number of occurrences used in average.

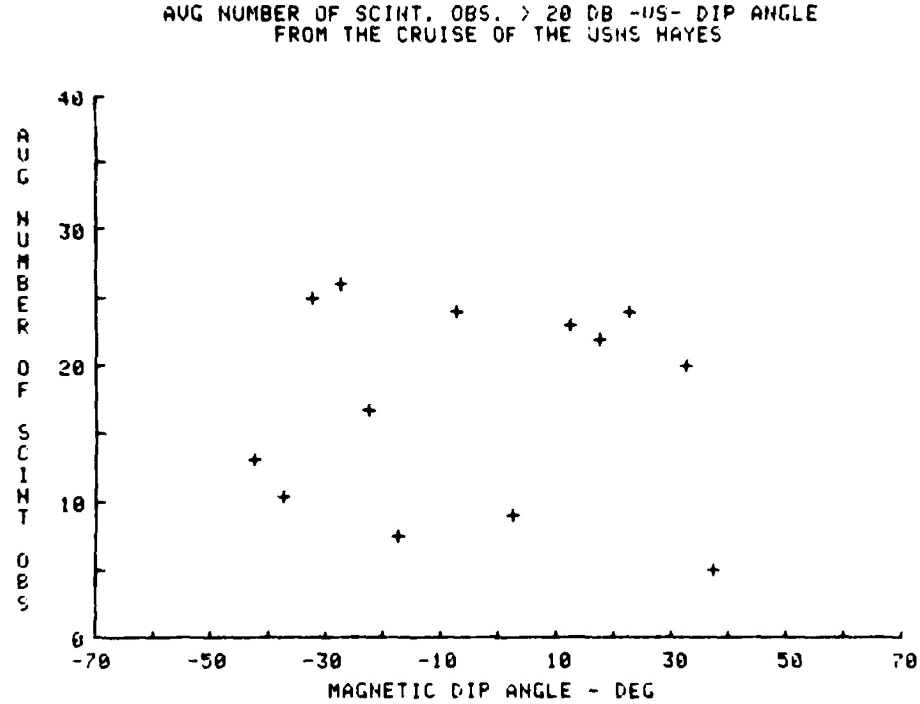

(A)

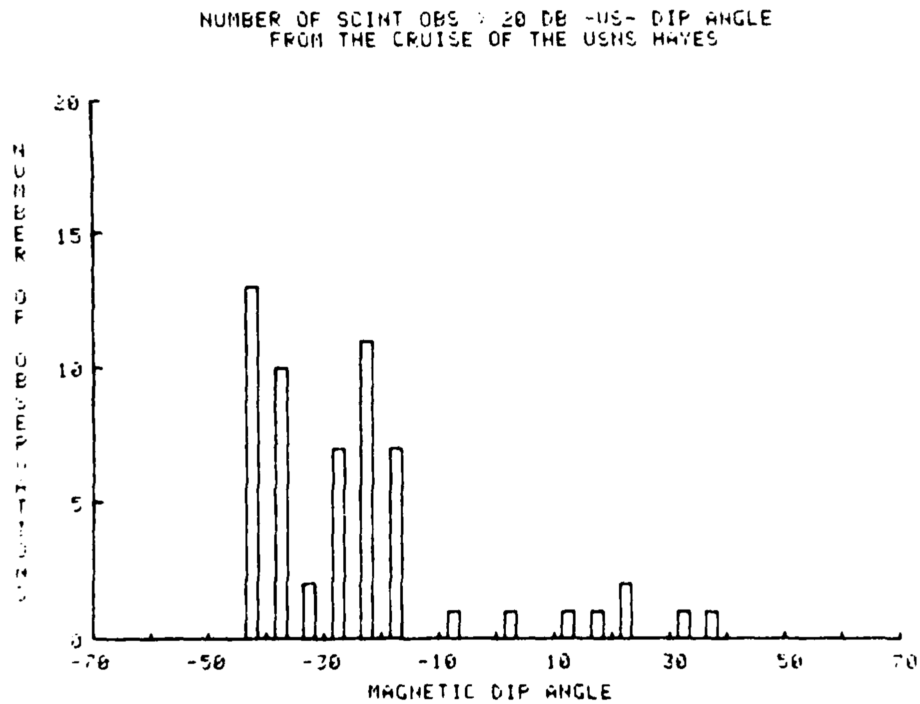

(B)

Fig. 19 - (A) Average maximum number of scintillation observations greater than 20 dB vs. dip angle.
(B) Number of occurrences used in average.

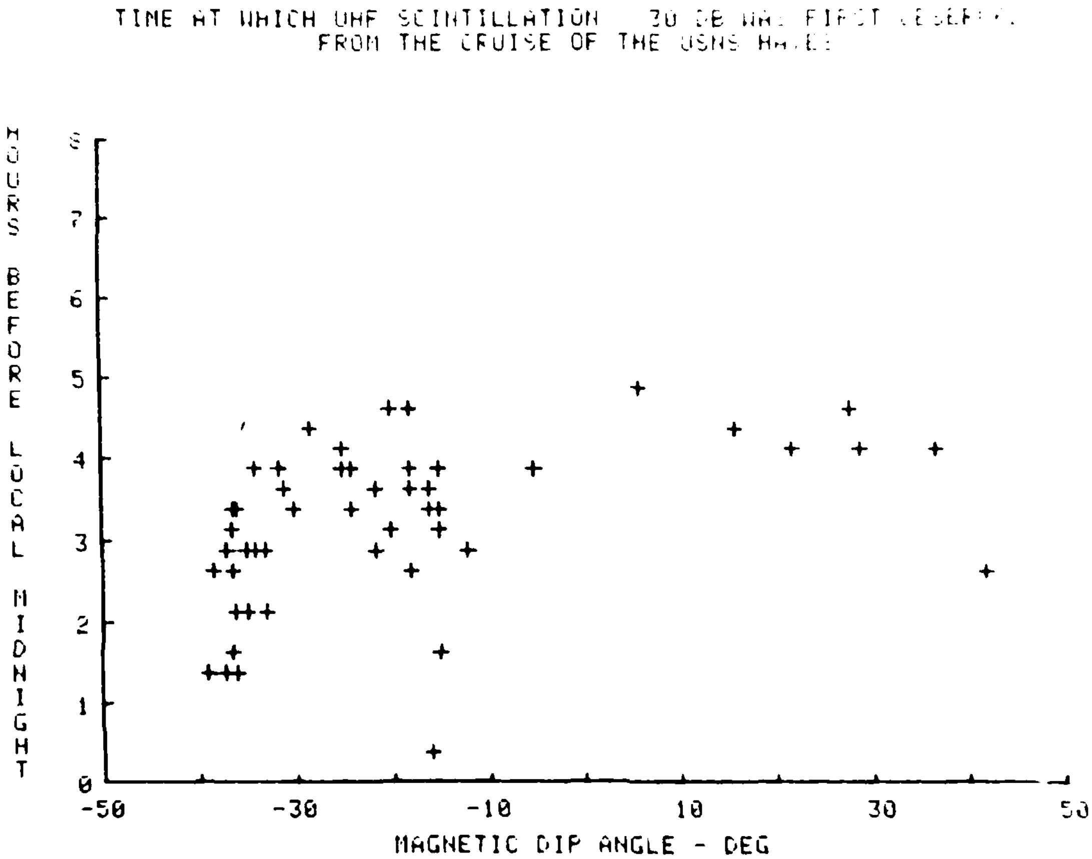

Fig. 20 - Time advance (prior to local midnight) at which 30 dB scintillation was observed

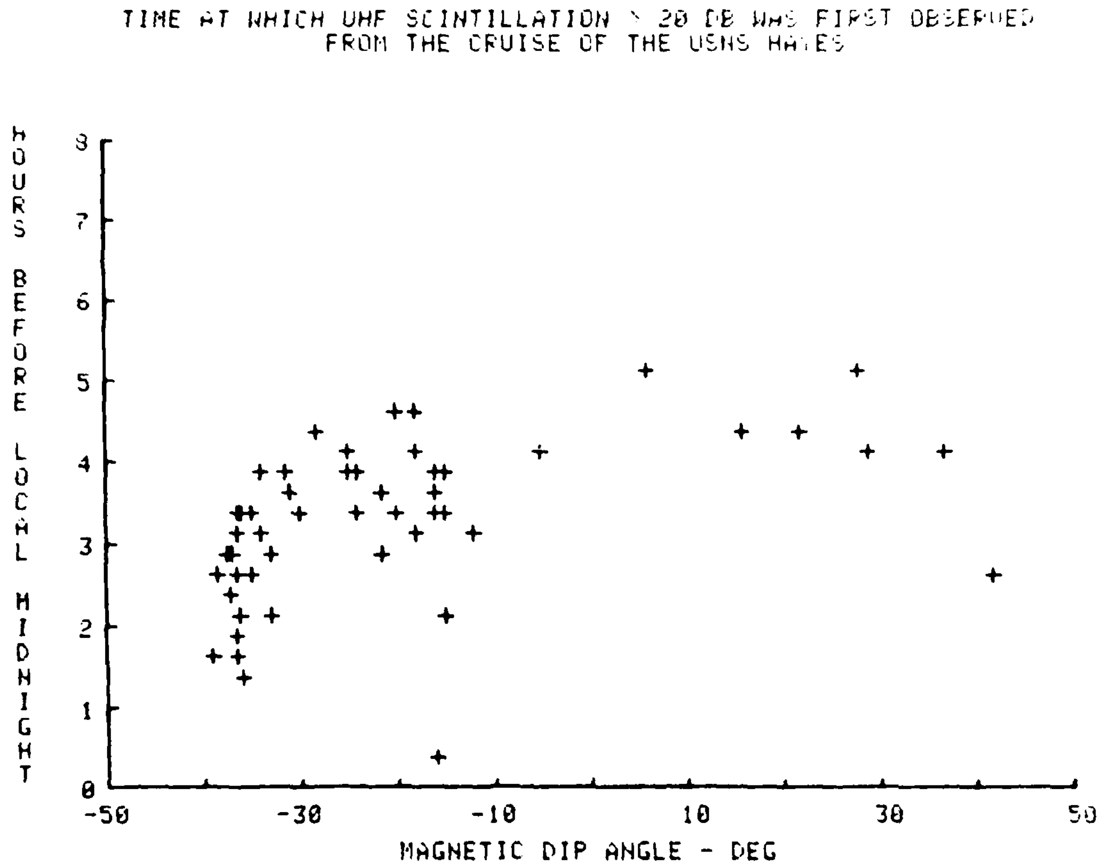

Fig. 21 - Time advance (prior to local midnight) at which 20 dB scintillation was observed

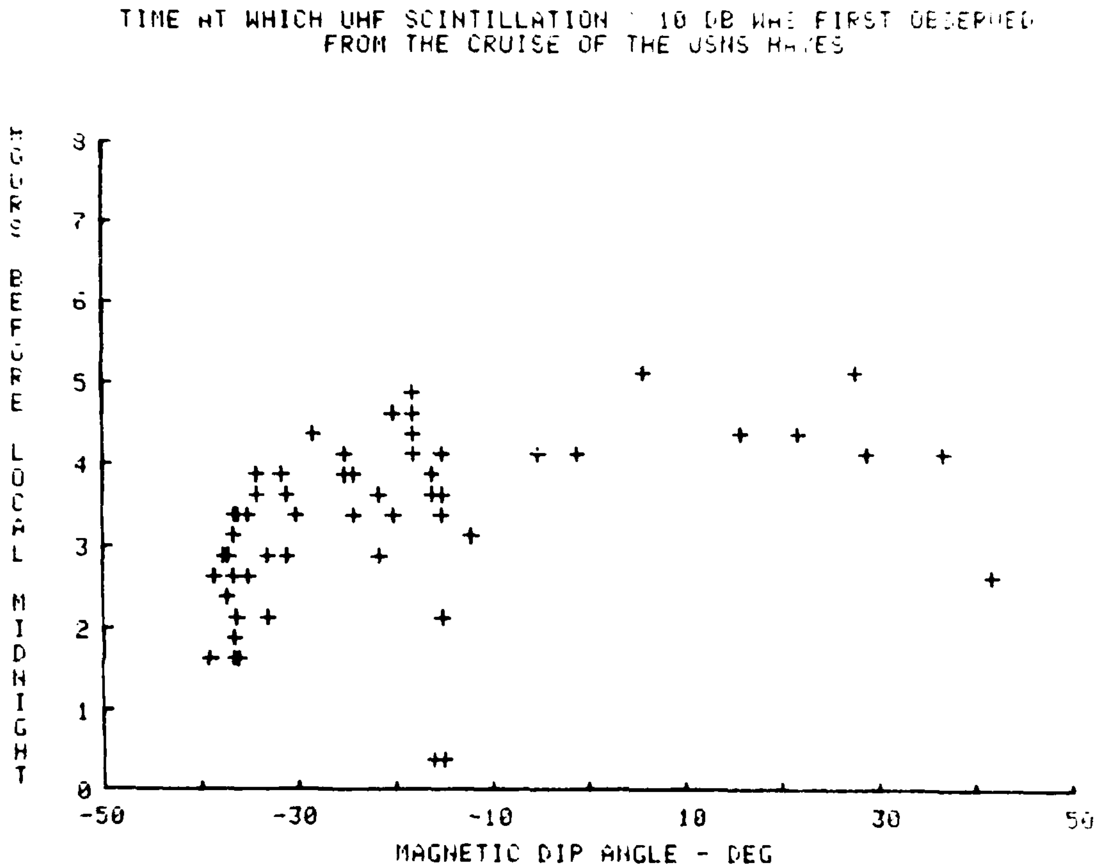

Fig. 22 - Time advance (prior to local midnight) at which 10 dB scintillation was observed

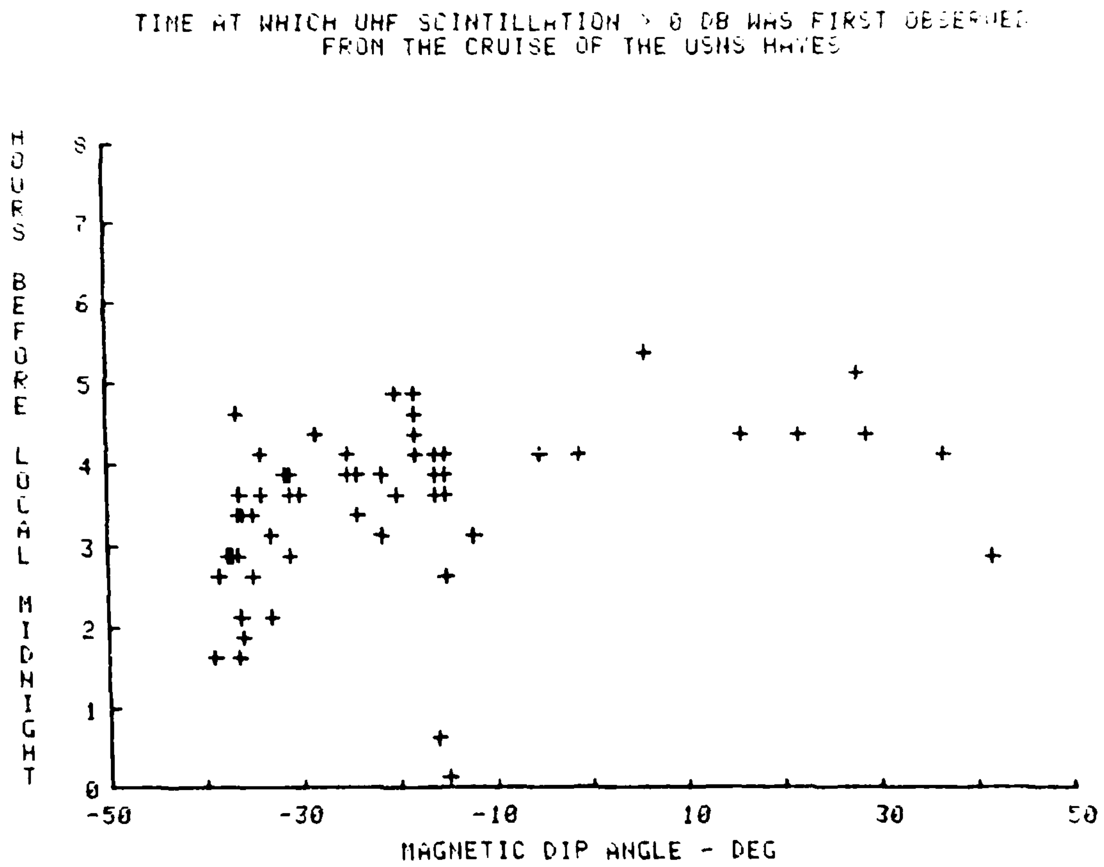

Fig. 23 - Time advance (prior to local midnight) at which 0 dB scintillation was observed

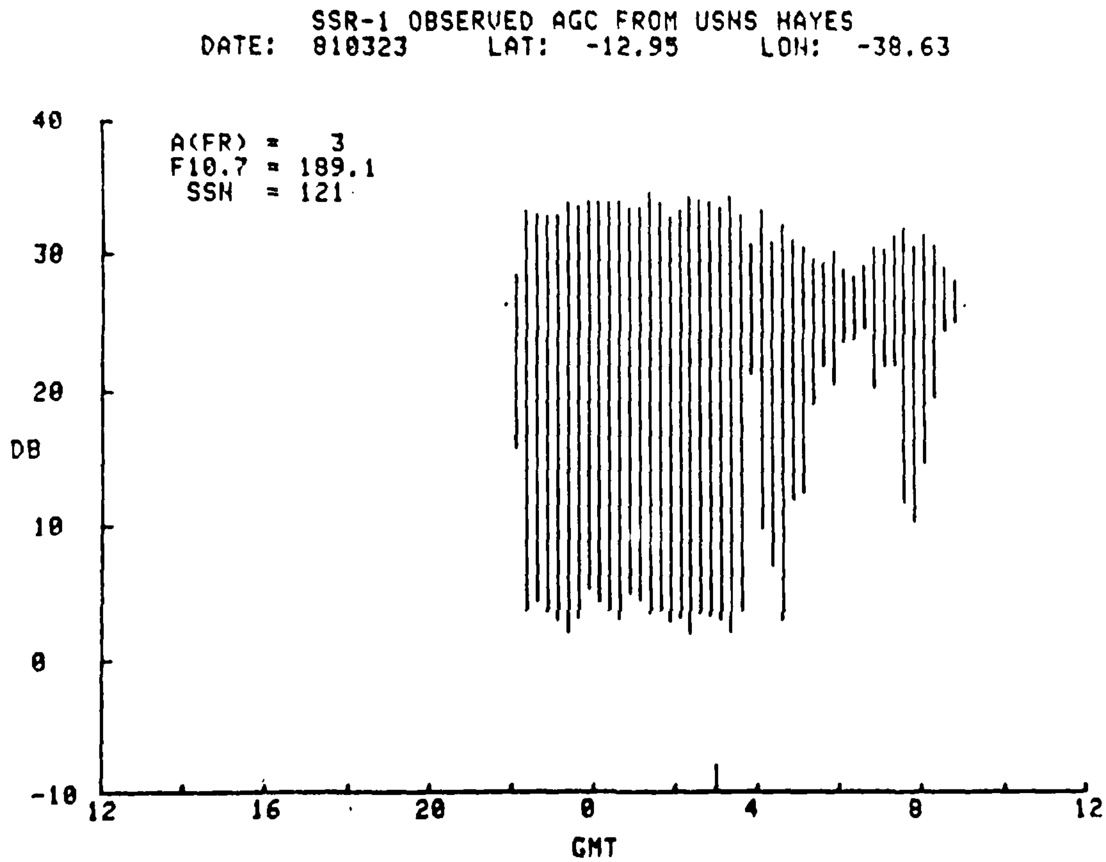

Fig. 24 - AGC level variations vs. GMT for March 23, 1981. The mean signal level is approximately 27 dB in this case (arbitrary dB scale).

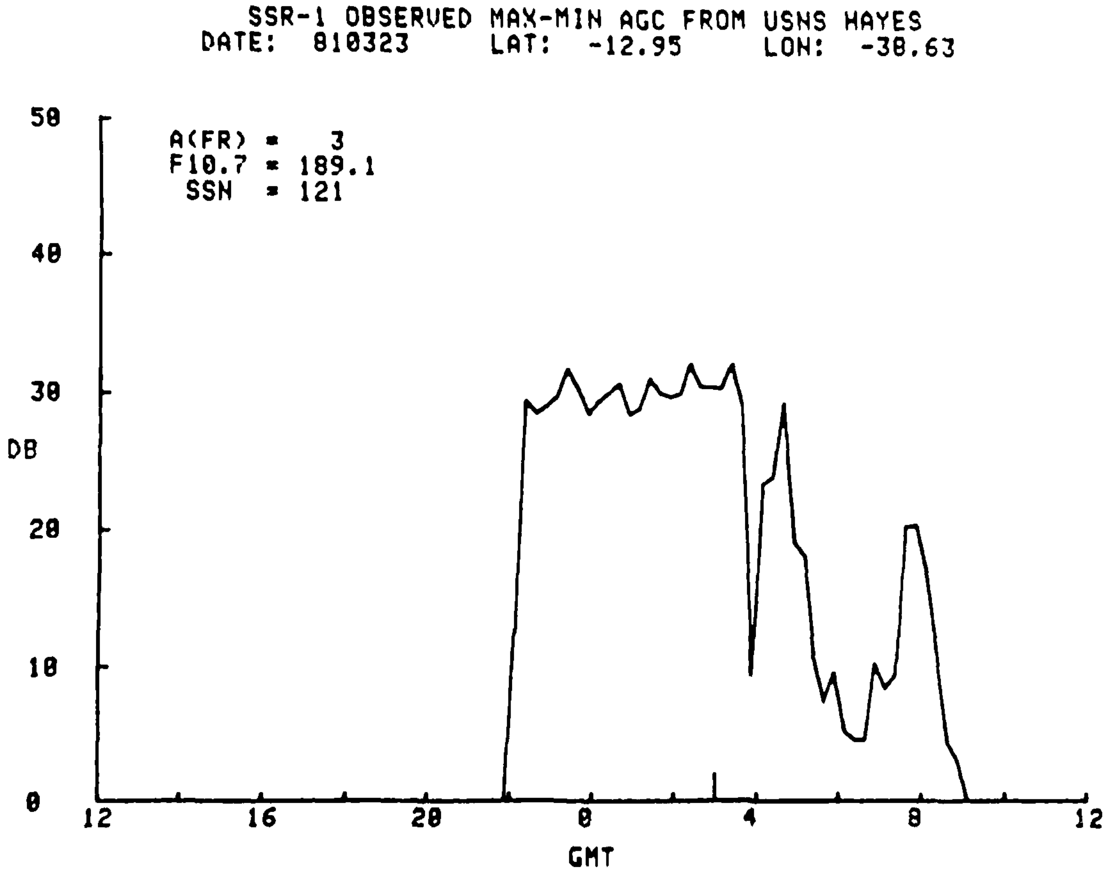

Fig. 25 - Range of AGC level variations (dB) versus GMT for 23 March 1981. The larger vertical "tick-mark" at 0300 GMT is local midnight. Note the sharp onset of scintillation approximately five (5) hours prior to midnight (shortly following sunset) and its gradual albeit erratic decay following midnight.

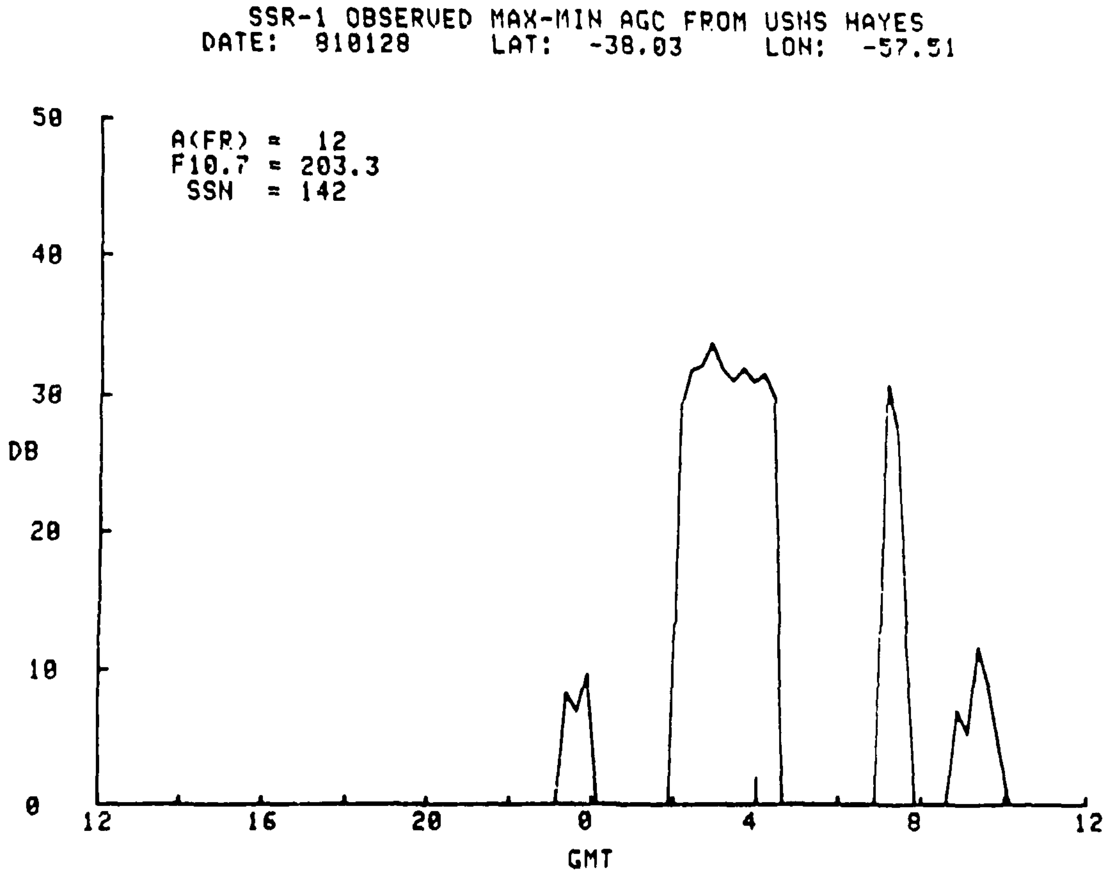

Fig. 26 - Same as Figure 25, except for January 28, 1981

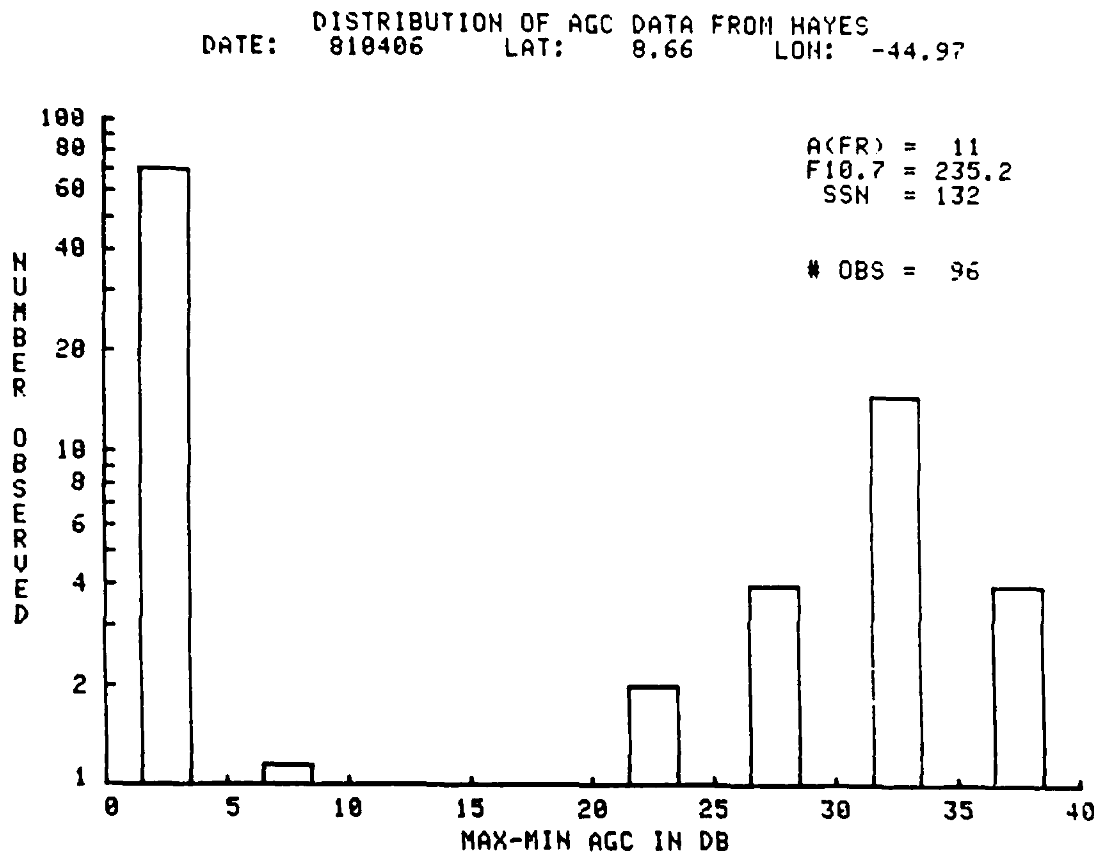

Fig. 27 - Distribution of fading depths for April 6, 1981

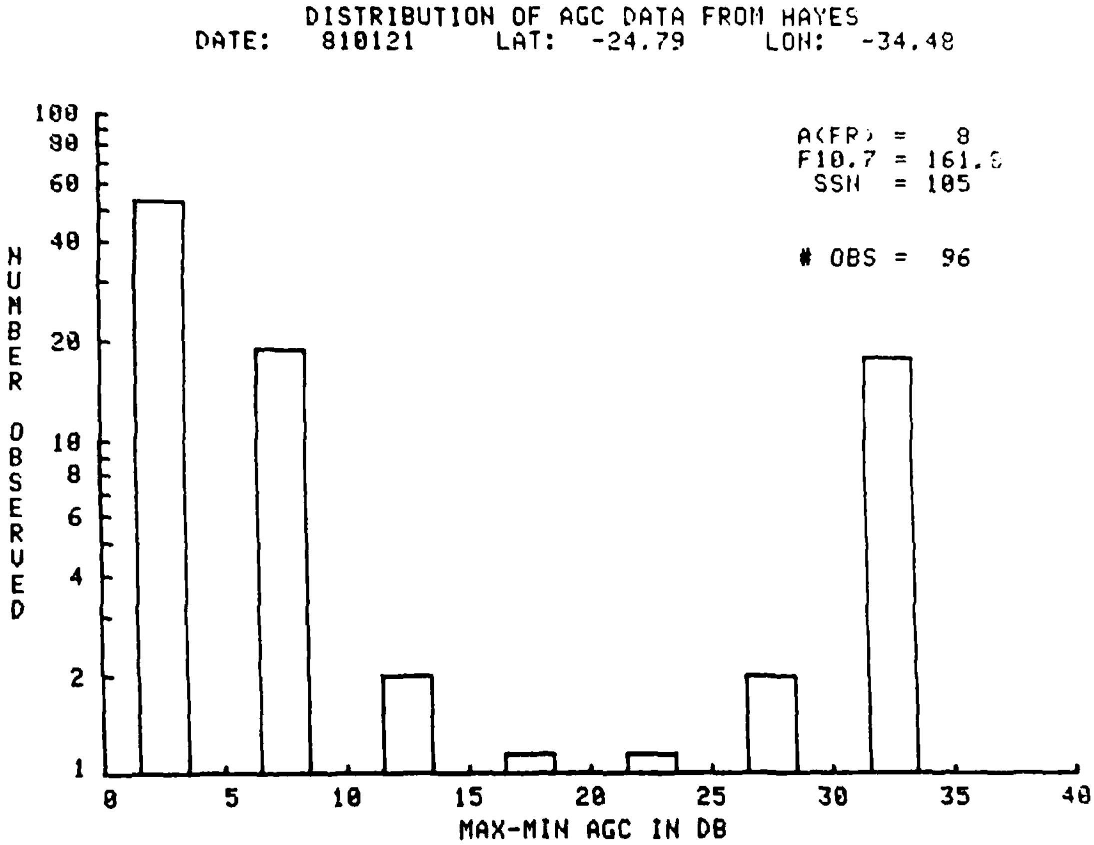

Fig. 28 - Distribution of fading depths for January 21, 1981

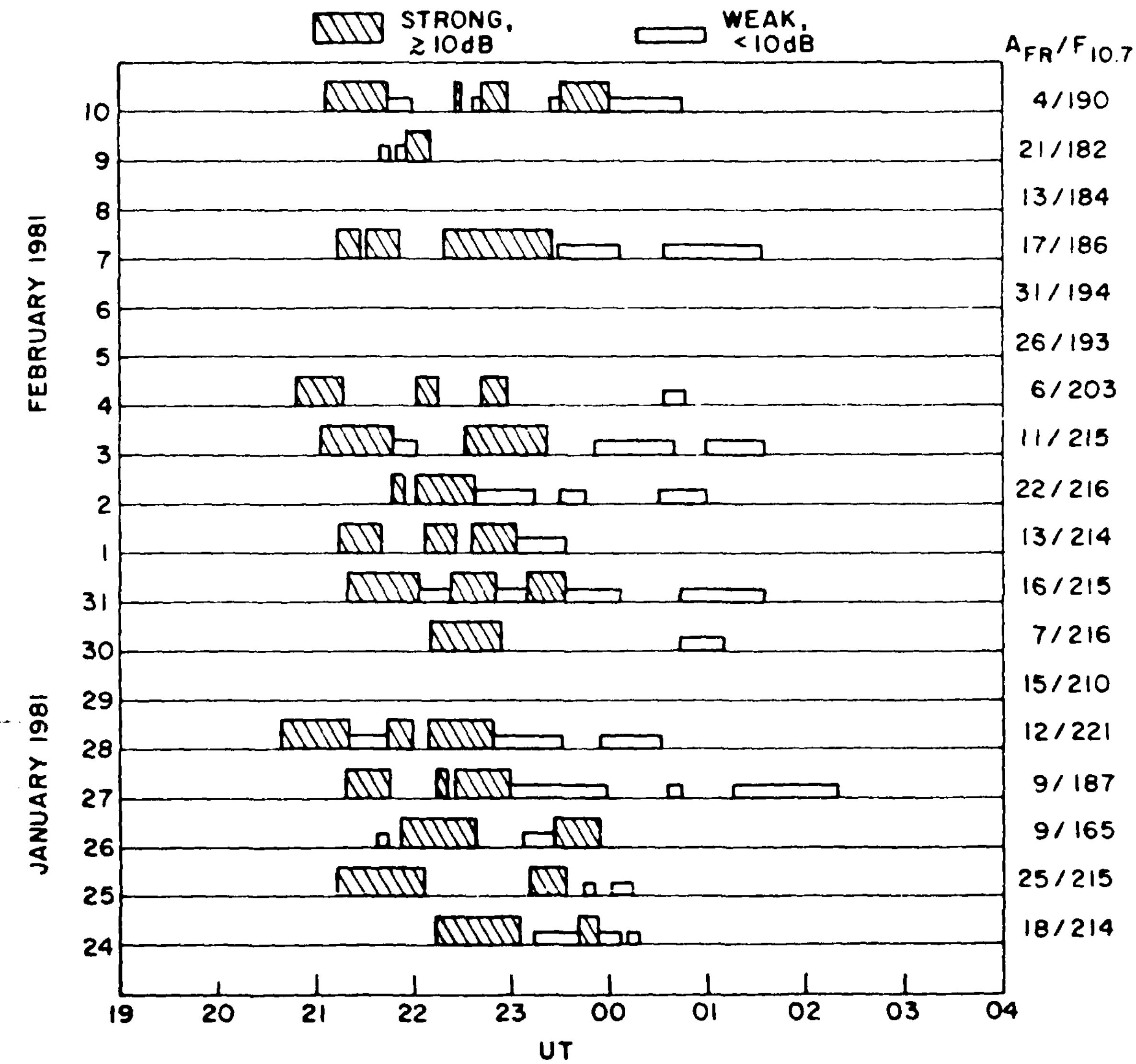

Fig. 29 - Occurrence of amplitude scintillation form Marisat (1541 MHz) Observed at Ascension Island (elevation 80.7°) courtesy J. Klobuchar, AFGL

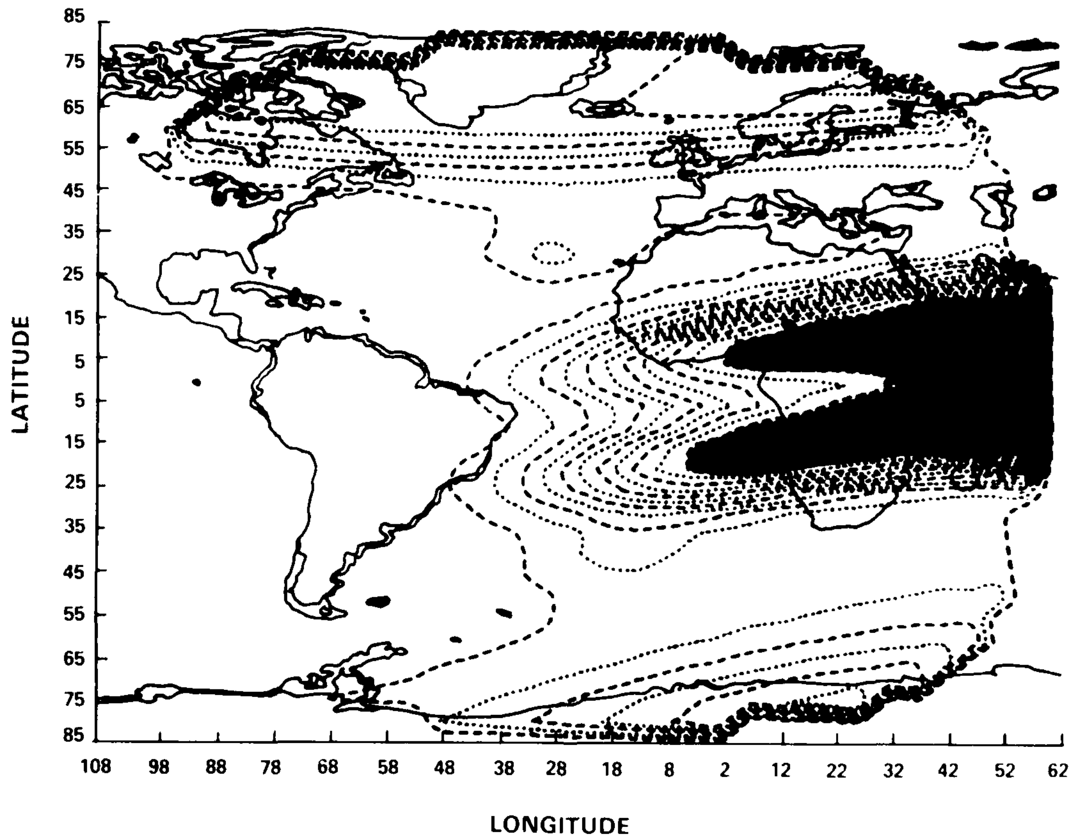

Fig. 30 - "Map" of UHF scintillation for 250 MHz transmissions from the Atlantic FLTSATCOM (23°W), under solar maximum conditions (15 Feb). The local time is approximately 2 hours following sunset at the sub-satellite point (2130 UT). (S_4 = 1 within the shaded region).

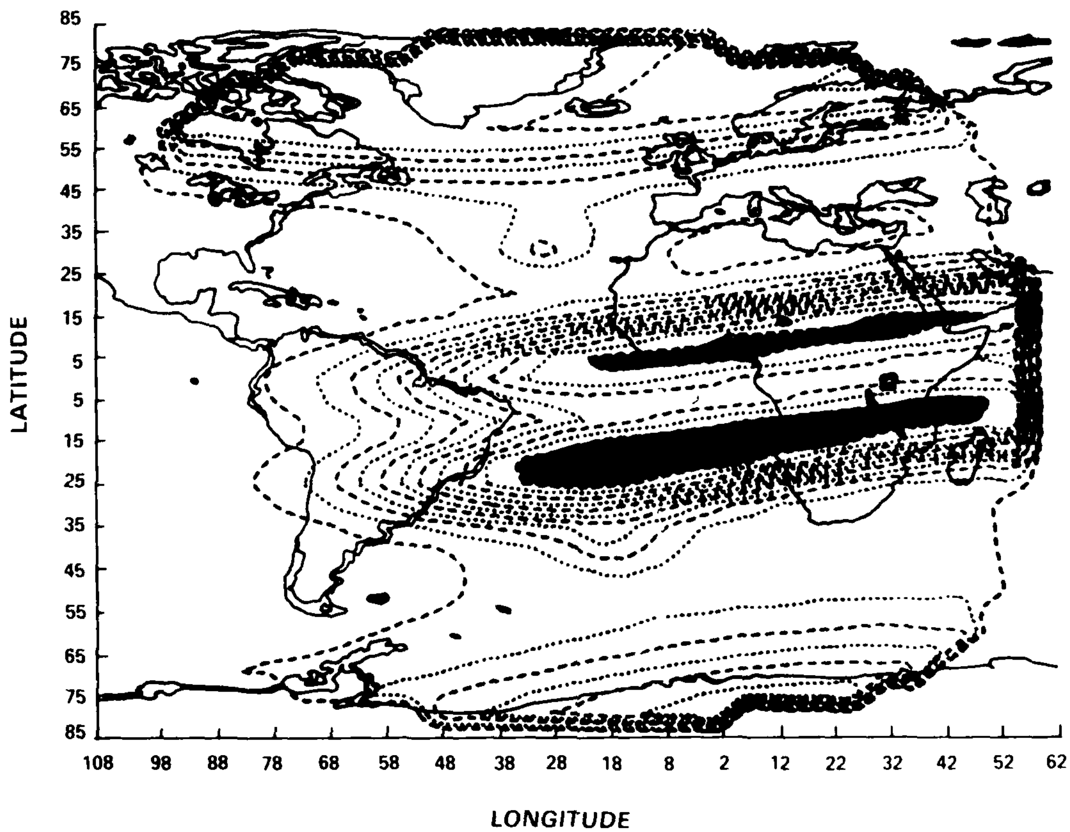

Fig. 31 - Same as 30, except the local time is about four hours after sunset at the subsatellite point (2330 UT)

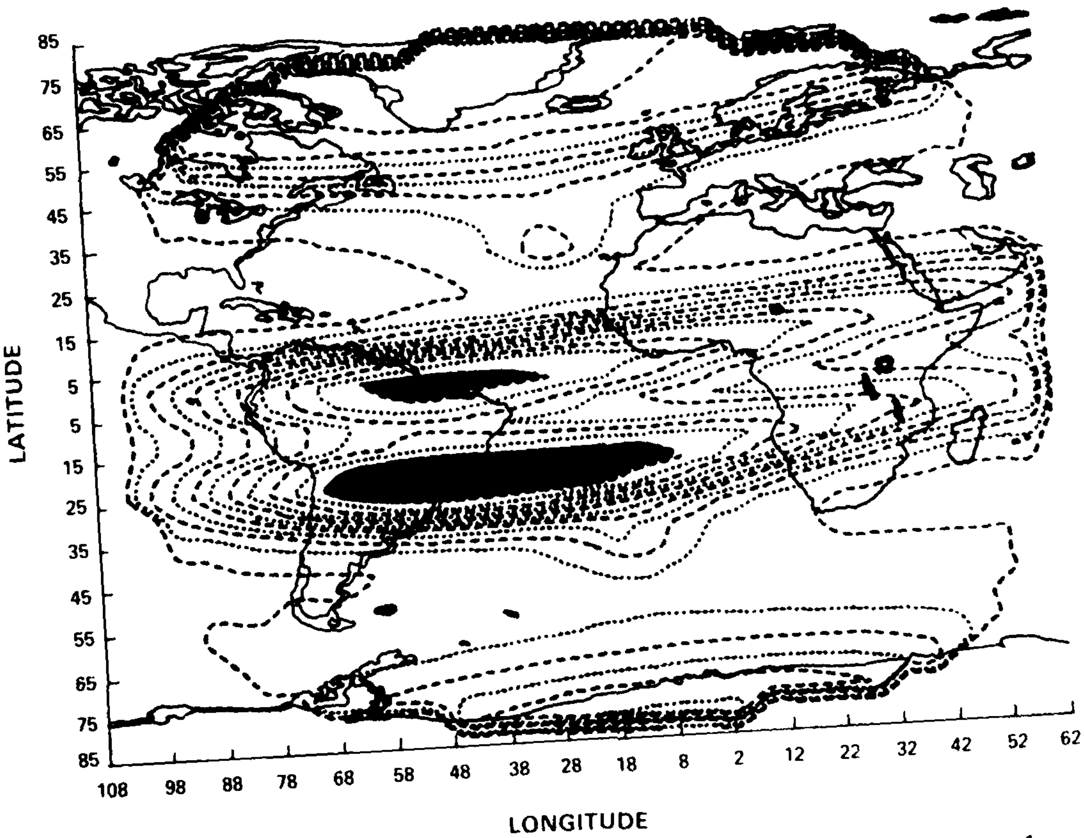

Fig. 32 - Same as 30 and 31, except the local time is approximately midnight at the subsatellite point (0130 UT)

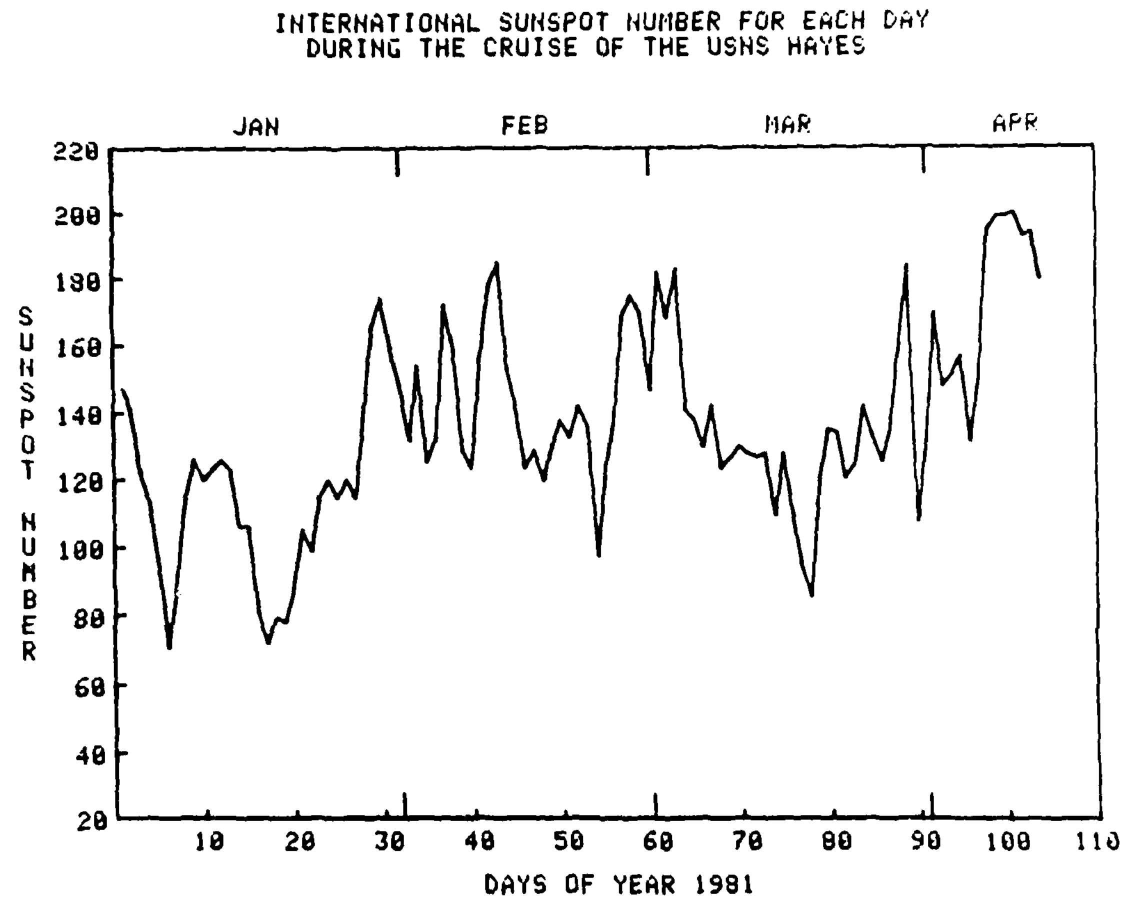

Fig. 33 - Sunspot number R_I vs. day of expedition

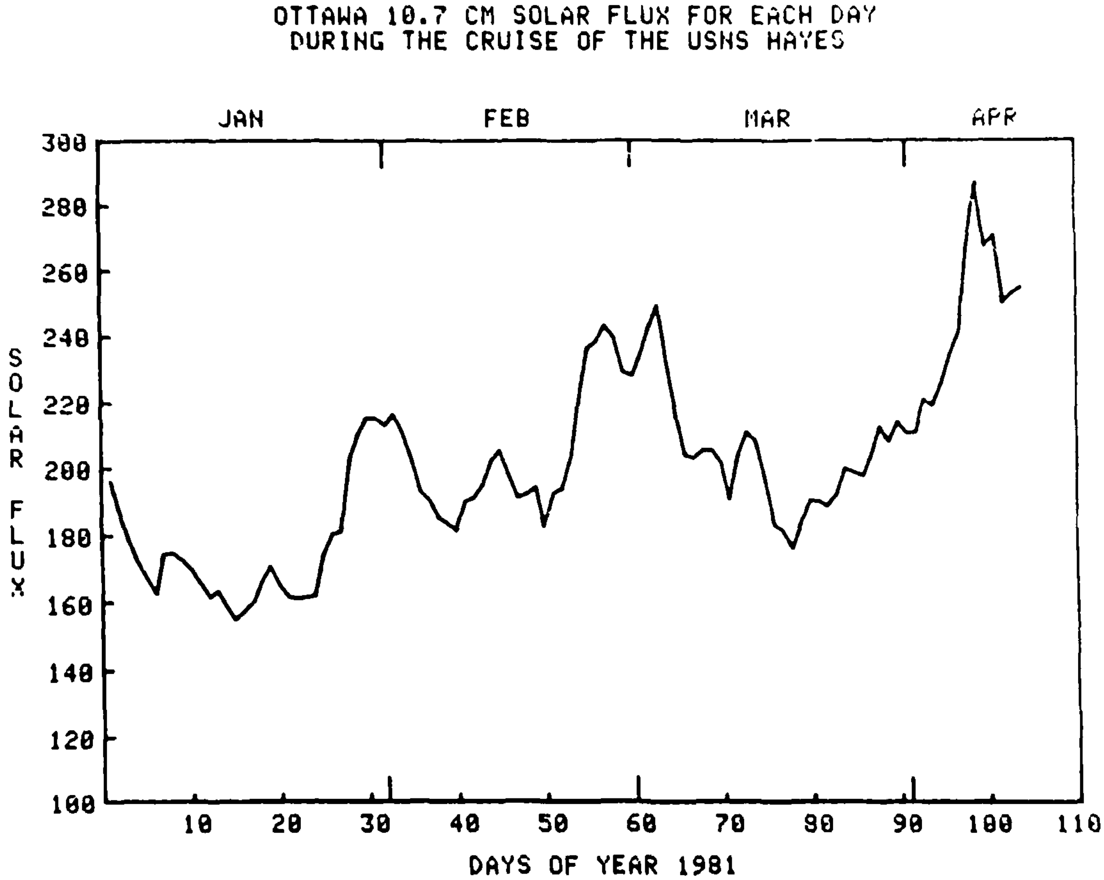

Fig. 34 - 10.7 cm solar flux vs. day of expedition

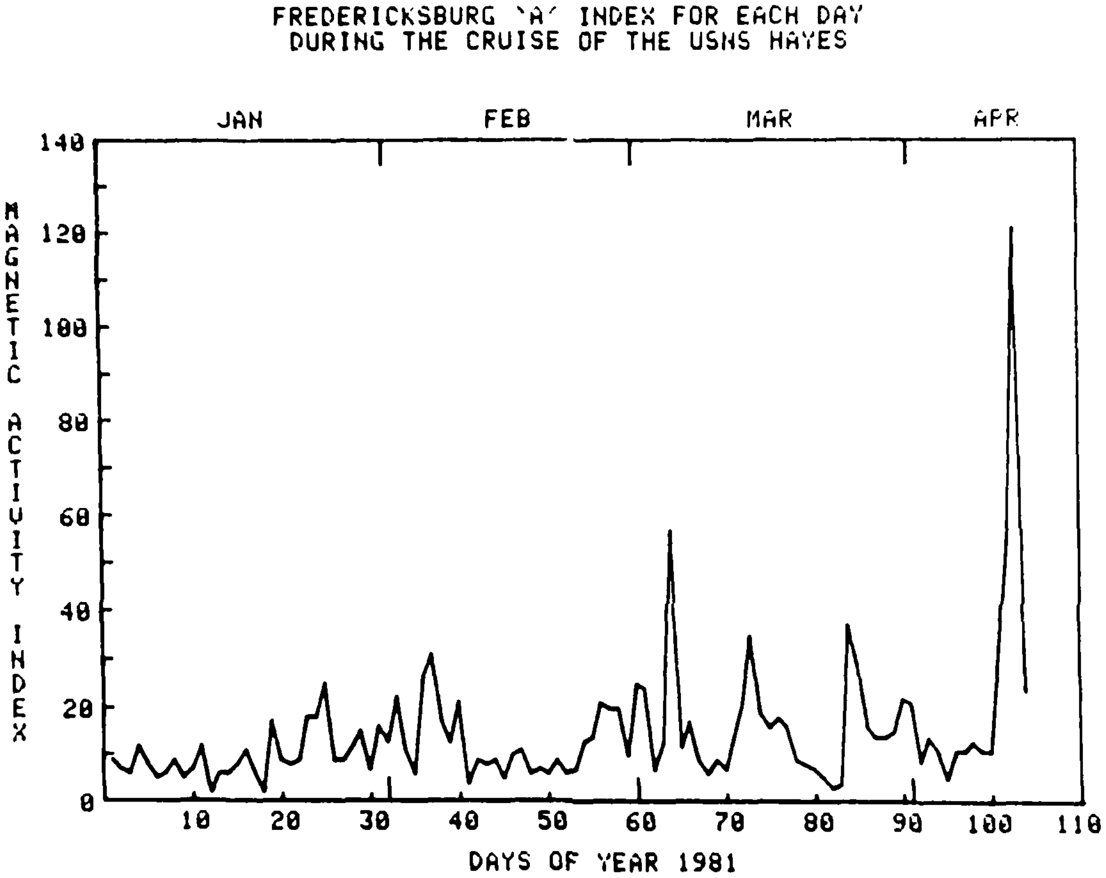

Fig. 35 - Magnetic activity index A_{FR} vs. day of expedition

Table 1 - Synopsis of data obtained during SOS '81

DATE	[illegible]	[illegible]	[illegible]	HDG	[illegible]	NRR OBS	[illegible]	% OF OBS BETWEEN INDICATED LEVELS								MAX EDGE	OER	10.7 FLUX	SSN	DIF ANGLE	AVG SLOPE	AVG EDGE
								[illegible]	[illegible]	10	15	[illegible]	[illegible]	[illegible]	[illegible]							
810101	12:00	[illegible]	[illegible]	[illegible]	12.?	96	0.0	96	0	0	0	0	0	0	0	[illegible]	9	19?.?	13?	61.0	[illegible]	[illegible]
[illegible]	12:00	[illegible]	[illegible]	[illegible]	13.9	96	0.0	96	0	0	0	0	0	0	0	[illegible]	[illegible]	18?.?	141	60.0	[illegible]	[illegible]
810103	12:00	[illegible]	[illegible]	[illegible]	11.?	96	0.0	96	0	0	0	0	0	0	0	[illegible]	[illegible]	17?.6	12?	58.?	0.00	0.00
810104	12:00	[illegible]	[illegible]	[illegible]	[illegible]	96	0.0	96	0	0	0	0	0	0	0	0.0	1?	1??.5	113	56.?	0.00	0.00
810105	12:00	[illegible]	[illegible]	[illegible]	1?.9	96	0.0	96	0	0	0	0	0	0	0	0.0	8	167.3	94	54.5	0.00	0.00
810106	[illegible]	[illegible]	[illegible]	15?	13.4	96	0.0	96	0	0	0	0	0	0	0	0.0	5	167.8	7?	49.0	0.00	0.00
810107	12:00	[illegible]	[illegible]	15?	[illegible]	96	40.8	90	0	1	0	1	3	1	0	26.1	4	174.1	89	47.0	1.69	1.35
810108	12:00	[illegible]	45.?	15?	13.4	96	31.3	69	5	2	[illegible]	1	1?	[illegible]	0	26.1	9	175.0	115	42.0	6.78	5.44
810109	12:00	13.1	[illegible]	[illegible]	13.?	96	32.6	69	1	2	1	1	17	6	0	24.8	5	172.7	126	28.0	7.62	5.62
810110	[illegible]	[illegible]	11.1	14?	1?.7	96	3?.9	65	3	3	[illegible]	1	1?	10	0	28.?	[illegible]	170.2	120	16.0	8.14	7.30
810111	[illegible]	[illegible]	[illegible]	14?	13.5	96	44.?	80	4	4	0	2	3	4	0	26.1	1?	166.0	123	6.0	4.54	3.58
810112	[illegible]	[illegible]	[illegible]	15?	[illegible]	96	41.5	65	2	5	0	2	11	11	0	26.1		161.9	126	-5.0	8.10	6.33
810113	[illegible]	1.?	[illegible]	[illegible]	[illegible]	96	41.3	75	[illegible]	[illegible]	2	6	2	4	0	23.?	6	163.5	123	-12.0	5.36	2.44
810114	[illegible]	[illegible]	[illegible]	[illegible]	[illegible]	96	26.3	63	4	1	4	5	12	1	0	23.5	6	159.2	106	-16.0	[illegible]	5.39
810115	[illegible]	[illegible]	[illegible]		0.0	96	[illegible]	75	1	1	1	3	15	0	0	21.1	8	154.9	106	-16.0	5.51	3.78
810116	[illegible]	[illegible]	[illegible]	[illegible]	[illegible]	96	[illegible]	60	3	4	2	1	8	15	1	25.8	11	157.5	81	16.0	9.15	6.89
810117	[illegible]	[illegible]	[illegible]		[illegible]	96	33.6	59	10	2	3	5	2	13	0	28.2	4	160.4	[illegible]	-10.0	7.89	6.11
810118	[illegible]	[illegible]	[illegible]	15?	12.5	96	[illegible]	62	14	0	1	1	0	14	4	28.2	2	164.3	[illegible]	24.0	8.45	6.17
810119	12:00	16.0	[illegible]	19?	13.6	96	[illegible]	[illegible]	4	0	0	1	3	1	1	26.5	17	170.9	78	33.0	6.06	4.41
810120	12:00	[illegible]	3?.5	197	13.?	96	36.5	64	2	1	2	1	0	19	5	28.8	9	165.?	89	46.0	9.41	7.30
810121	12:00	4.9	[illegible]	109	13.7	96	34.2	57	19	2	1	1	2	18	0	27.7	8	161.8	105	-38.5	8.83	6.99
810122	12:00	[illegible]	[illegible]	20	13.4	96	33.4	81	2	0	0	1	1	11	0	25.1	9	161.4	99	-29.0	4.36	3.18
810123	12:00	31.?	29.5	31?	4.8	96	0.0	96	0	0	0	0	0	0	0	0.0	18	161.8	115	-48.0	0.00	0.00
810124	12:00	33.3	4?.9	[illegible]	1?.1	96	33.5	60	6	2	[illegible]	0	11	9	0	25.8	18	16?.3	120	37.?	8.07	6.23
810125	12:00	41.3	[illegible]	[illegible]	1?.9	96	31.4	89		3	0	0	1	2	0	23.3	25	174.6	115	-36.0	1.46	1.01
810126	12:00	[illegible]	[illegible]	23?	15.3	96	34.?	76	1	1	0	2	2	9	0	2?.6	9	180.?	120	-36.2	[illegible]	4.35
810127	12:00	38.0	5?.5	0	0.0	96	33.4	81	3	1	0	0	1	10	0	25.2	9	181.2	115	36.5	4.17	3.03
810128	[illegible]	[illegible]	5?.5	0	0.0	96	34.0	74	6	2	0	0	3	9	0	26.0	1?	207.3	142	36.5	4.70	3.63
810129	[illegible]	[illegible]	[illegible]	0	0.0	96	33.2	73	3	2	2	1	1	12	0	28.1	15	210.5	165	-34.5	5.38	4.23
810130	[illegible]	[illegible]	[illegible]	0	0.0	96	2?.9	65	6	4	4	2	6	8	1	[illegible]		215.6	174	-36.5	6.99	5.37
810131	[illegible]	[illegible]	[illegible]	0	0.0	96	0.0	96	0	0	0	0	0	0	0	0.0	16	215.3	159	-36.5	0.00	0.00
810201	12:00	[illegible]	[illegible]	0	0.0	96	0.0	96	0	0	0	0	0	0	0	0.0	13	213.5	148	37.7	0.00	0.00
810202	12:00	29.3	[illegible]	0	13.?	96	0.0	96	0	0	0	0	0	0	0	0.0	22	216.4	132	-29.?	0.00	0.00
810203	12:00	31.?	[illegible]	[illegible]	13.?	96	0.0	96	0	0	0	0	0	0	0	0.0	11	211.5	154	41.5	0.00	0.00
810204	12:00	44.?	[illegible]	[illegible]	9.8	96	0.0	96	0	0	0	0	0	0	0	0.0	6	203.2	126	-43.5	0.00	0.00
810205	12:00	[illegible]	55.5	17?	13.?	96	0.0	96	0	0	0	0	0	0	0	0.0	16	193.2	133	-46.2	0.00	0.00
810206	12:00	[illegible]	[illegible]	15?	13.?	96	0.0	96	0	0	0	0	0	0	0	0.0	31	190.7	172	-49.5	0.00	0.00
810207	12:00	[illegible]	[illegible]	17?	13.1	96	0.0	96	0	0	0	0	0	0	0	0.0	17	18?.5	158	-51.0	0.00	0.00
810208	12:00	[illegible]	49.0	15?	11.2	96	0.0	96	0	0	0	0	0	0	0	0.0	13	184.1	129	-53.2	0.00	0.00
810209	12:00	[illegible]	47.?	[illegible]	13.?	96	0.0	96	0	0		0	0	0	0	0.0	11	181.6	124	-53.2	0.00	0.00
810210	12:00	[illegible]	[illegible]	[illegible]	1?.8	96	0.0	96	0	0	0	0	0	0	0	0.0	4	190.1	15?	-52.0	0.00	0.00
810211	12:00	[illegible]	[illegible]	[illegible]	1?.6	96	0.0	96	0	0	0	0	0	0	0	0.0	9	191.4	178	56.5	0.00	0.00
810212	12:00	49.?	[illegible]		[illegible]	96	0.0	96	0	0	0	0	0	0	0	0.0	8	19?.7	18?	48.1	0.00	0.00
810213	12:00	[illegible]	4?.8	[illegible]	[illegible]	96	0.0	96	0	0	0	0	0	0	0	0.0	9	202.9	15?	46.5	0.00	0.00
810214	12:00	[illegible]	38.9	113	1?.7	96	0.0	96	0	0	0	0	0	0	0	0.0	5	20?.4	142	-43.7	0.00	0.00
810215	12:00	19.?	[illegible]	12?	11.3	96	0.0	96	0	0	0	0	0	0	0	0.0	10	198.5	124	42.5	0.00	0.00
810216	12:00	41.?	[illegible]	[illegible]	14.5	96	0.0	96	0	0	0	0	0	0	0	0.0	11	191.5	129	-40.7	0.00	0.00
810217	12:00	[illegible]	45.?	[illegible]	13.4	96	0.0	96	0	0	0	0	0	0	0	0.0	6	19?.7	120	[illegible]	0.00	0.00
810218	12:00	44.?	[illegible]		11.?	96	33.4	76	1	2	2	0	1	9	0	[illegible]	[illegible]	194.?	131	-3?.0	4.58	3.5?
810219	12:00	26.?	[illegible]		[illegible]	[illegible]	33.4	65	[illegible]	0	0	0	0	4	0	25.0	6	183.0	139	-36.3	?.04	1.51
810220	12:00	28.0	[illegible]		[illegible]	96	0.0	96	0	0	0	0	0	0	0	0.0	9	19?.5	133	-37.0	0.00	0.00
810221	12:00	25.1	[illegible]		13.?	96	34.?	90	2	1	0	0	0	2	1	28.4	6	194.2	14?	-34.0	1.37	1.01
810222	12:00	41.?	49.1	[illegible]	1?.5	96	33.4	9?	0	0	0	0	1	3	0	25.6	[illegible]	204.0	136	-34.0	1.34	1.03
810223	12:00	[illegible]	[illegible]	3?	1?.8	96	29.4	8?	1	0	[illegible]	1	1	4	3	40.8	17	[illegible]	98	31.?	[illegible]	2.44
810224	12:00	4.1	41.?	[illegible]	13.?	96	34.8	9?	1	0	0	0	[illegible]	1	[illegible]	[illegible]	14	[illegible]	1?4	31.?	[illegible]	1.01

Table 1 (Cont'd) - Synopsis of data obtained during SOS '81

DATE	GMT	LAT	LON	HDG	SPD	NBR OBS	MAX SCNT	# OF OBS BETWEEN INDICATED LEVELS 00	05	10	15	20	25	30	35 40	MAX FADE	AK	10.7 FLUX	SSN	DIP ANGLE	AVG SCINT	AVG FADE
810225	12:00	19.5	48.9	21	13.0	96	0.0	96	0	0	0	0	0	0	0	0.0	21	238.6	[illegible]	-24.2	0.00	0.00
810226	12:00	14.6	39.5	[illegible]	13.0	96	33.6	92	1	0	0	0	0	3	0	17.5	20	243.4	169	18.0	1.13	0.88
810227	12:00	13.0	-38.6	[illegible]	0.0	96	[illegible]	83	0	2	0	1	2	8	0	25.3	20	240.0	175	-18.0	3.81	[illegible]
810228	12:00	13.0	-48.6	[illegible]	0.0	44	0.0	44	0	0	0	0	0	0	0	0.0	10	229.3	170	-18.0	0.00	0.00
810301	12:00	13.2	38.5	[illegible]	0.0	[illegible]	38.2	[illegible]	1	1	0	0	0	13	6	28.6	25	228.5	147	-20.0	7.20	5.35
810302	12:00	-12.9	[illegible]	[illegible]	7.5	96	[illegible]	60	2	3	1	2	3	17	8	29.4	24	234.6	182	-21.5	11.06	8.57
810303	12:00	[illegible]	34.0	84	[illegible]	96	[illegible]	[illegible]	10	4	1	[illegible]	4	16	4	29.4	7	243.0	169	-24.0	8.73	6.46
810304	12:00	[illegible]	[illegible]	114	[illegible]	96	[illegible]	[illegible]	4	1	3	0	0	[illegible]	[illegible]	18.9	13	249.6	184	24.0	9.78	7.44
810305	12:00	13.2	[illegible]	113	8.8	96	0.0	96	0	0	0	0	0	0	0	0.0	57	231.0	141	-25.0	0.00	0.00
810306	12:00	[illegible]	[illegible]	123	7.6	96	[illegible]	60	3	1	2	1	3	18	8	18.9	12	215.9	138	-25.0	10.86	8.38
810307	12:00	14.0	-30.9	136	[illegible]	96	[illegible]	96	0	0	0	0	0	0	0	0.0	17	204.5	130	-28.0	0.00	0.00
810308	12:00	[illegible]	-29.8	18	[illegible]	96	37.1	[illegible]	4	4	2	4	3	21	5	18.8	9	204.4	142	-25.0	[illegible]	9.52
810309	12:00	13.4	29.4	176	8.8	[illegible]	38.1	58	5	4	2	1	1	10	15	40.3	6	205.8	124	-28.2	10.89	8.31
810310	12:00	12.2	[illegible]	[illegible]	8.4	96	[illegible]	71	4	1	0	0	3	11	6	19.0	9	205.8	127	31.0	7.60	5.81
810311	12:00	13.0	27.0	[illegible]	9.0	96	35.6	66	3	2	2	0	3	18	2	28.2	7	202.3	130	-39.0	8.85	6.83
810312	12:00	14.1	[illegible]	144	7.6	96	[illegible]	69	4	0	0	0	[illegible]	11	8	29.4	14	191.1	128	31.5	7.89	6.08
810313	12:00	[illegible]	4.3	120	8.3	96	34.3	[illegible]	0	1	1	0	1	6	2	29.0	21	204.6	[illegible]	-44.0	[illegible]	2.74
810314	12:00	12.3	[illegible]	[illegible]	8.4	96	0.0	96	0	0	0	0	0	0	0	0.0	35	[illegible]	[illegible]	[illegible]	0.00	0.00
810315	12:00	[illegible]	[illegible]	[illegible]	8.1	96	[illegible]	80	2	1	0	0	3	6	4	[illegible]	19	[illegible]	110	[illegible]	4.64	3.60
810316	12:00	12.9	-19.3	[illegible]	8.5	96	[illegible]	94	0	0	0	0	[illegible]	0	0	21.4	16	196.5	[illegible]	-37.5	0.60	0.44
810317	12:00	13.9	21.1	140	8.9	96	[illegible]	92	0	0	0	0	[illegible]	[illegible]	0	25.0	15	187.3	109	-45.0	1.28	0.92
810318	12:00	14.1	[illegible]	[illegible]	9.0	96	13.5	94	1	1	0	0	0	0	0	[illegible]	16	181.6	95	-31.0	0.24	0.14
810319	12:00	[illegible]	28.0	[illegible]	8.8	96	0.0	96	0	0	0	0	0	0	0	0.0	5	174.5	86	[illegible]	0.00	0.00
810320	12:00	[illegible]	[illegible]	[illegible]	14.0	96	[illegible]	[illegible]	[illegible]	1	4	[illegible]	0	[illegible]	5	[illegible]	[illegible]	[illegible]	120	[illegible]	9.12	6.96
810321	12:00	[illegible]	[illegible]	[illegible]	0.0	96	0.0	96	0	0	0	0	0	0	0	0.0	[illegible]	[illegible]	135	18.0	0.00	0.00
[illegible]	12:00	[illegible]	[illegible]	[illegible]	0.0	[illegible]	[illegible]	78	1	0	1	4	3	9	0	[illegible]	5	190.7	134	18.0	5.13	[illegible]
810323	12:00	[illegible]	[illegible]	[illegible]	0.0	[illegible]	[illegible]	56	6	4	3	4	11	12	0	14.4	[illegible]	189.1	121	18.0	9.86	[illegible]
810324	12:00	[illegible]	[illegible]	[illegible]	[illegible]	[illegible]	[illegible]	74	0	2	0	0	1	8	11	[illegible]	4	192.6	125	18.0	7.45	5.73
810325	12:00	11.0	[illegible]	[illegible]	11.6	[illegible]	[illegible]	[illegible]	[illegible]	0	0	0	0	[illegible]	[illegible]	[illegible]	[illegible]	[illegible]	142	16.0	[illegible]	[illegible]
[illegible]	[illegible]	[illegible]	[illegible]	[illegible]	[illegible]	[illegible]	[illegible]	[illegible]	[illegible]	1	[illegible]	1	[illegible]	[illegible]	[illegible]	[illegible]	[illegible]	[illegible]	[illegible]	[illegible]	1.85	1.44
[illegible]	[illegible]	[illegible]	[illegible]	[illegible]	[illegible]	[illegible]	[illegible]	[illegible]	[illegible]	1	1	[illegible]	[illegible]	[illegible]	[illegible]	[illegible]	[illegible]	[illegible]	[illegible]	[illegible]	[illegible]	[illegible]
[illegible]	[illegible]	[illegible]	[illegible]	[illegible]	[illegible]	[illegible]	[illegible]	[illegible]	[illegible]	[illegible]	1	[illegible]	[illegible]	[illegible]	[illegible]	[illegible]	[illegible]	[illegible]	[illegible]	[illegible]	[illegible]	[illegible]
[illegible]	[illegible]	[illegible]	[illegible]	[illegible]	[illegible]	[illegible]	[illegible]	[illegible]	1	1	[illegible]	1	[illegible]	[illegible]	[illegible]	[illegible]	14	[illegible]	[illegible]	[illegible]	[illegible]	[illegible]
[illegible]	[illegible]	[illegible]	[illegible]	[illegible]	[illegible]	[illegible]	[illegible]	[illegible]	[illegible]	[illegible]	[illegible]	[illegible]	[illegible]	[illegible]	[illegible]	[illegible]	[illegible]	[illegible]	[illegible]	[illegible]	[illegible]	[illegible]
[illegible]	[illegible]	[illegible]	[illegible]	[illegible]	[illegible]	[illegible]	[illegible]	[illegible]	[illegible]	[illegible]	[illegible]	[illegible]	[illegible]	[illegible]	[illegible]	[illegible]	[illegible]	[illegible]	[illegible]	[illegible]	[illegible]	[illegible]

REFERENCES

1. Aarons J., 1978, "Ionospheric Scintillations - An Introduction" in Recent Advances in Radio and Optical Propagation for Modern Communications, Navigation, and Detection Systems edited by J. Aarons, AGARD-LS-93, Tech. Edit. and Reprod. Ltd., London.

2. Aarons J., H.E. Whitney, E. MacKenzie, and S. Basu, 1981, Radio Sci., 15 (in press).

3. Anderson D.N., 1973, J. Planet. Space Sci., 21, 421.

4. Appleton E.V., 1946, Nature 157, 691.

5. Basu S. and S. Basu, 1981, J. Atmospheric Terrest. Phys. 43, (5/6) 473-489.

6. Basu S. and M.C. Kelley, 1979, Radio Sci., 14, 471.

7. Ben'kova N.P., K.N. Vasil'yer, O.P. Kitomiytsev, and J.S. Prutenskiy, 1978, Geomag. and Aeron. 18 (6) 704.

8. Benson R.F., 1981, URSI General Assembly paper.

9. Crane R.K., 1974, "Morphology of Ionospheric Scintillation", Lincoln Lab TN-1974-29.

10. Dyson P.L. and R.F. Benson, 1978, Geophys. Res. Lett. 5, 795.

11. Fejer B.G., 1981, J. Atmospheric Terrest. Phys., 43, 5-6, 377.

12. Fejer B.G., D.T. Farley, R.F. Woodman, and C. Calderon, 1979, J. Geophys. Res., 84 (A10) 5792.

13. Fremouw E.J. and C.L. Rino, 1978, "A Signal Statistical and Morphological Model of Ionospheric Scintillation" in Operational Modelling of the Aerospace Propagation Environment edited by H. Soicher, AGARD-CP-238., Tech. Edit. and Reprod. Ltd., London.

14. Goodman J.M., 1980, "A Resume of Anticipated FLEETSATCOM and GAPFILLER Scintillation Effects During the Peak of Solar Activity 1980-1982," in Vol. 4 Solar-Terrestrial Predictions Proceedings edited by R.F. Donnelly, pp D1-D50, US Gov't Printing Office, Washington, D. C.

15. Heelis R.A., P.C. Kendall, R.J. Moffett, D.W. Windle, and H. Rishbeth, 1974, Planet. Space Sci., 22, 743.

16. Kelley M.C., and J.P. McClure, 1981, J. Atmospheric Terrest. Phys. 43, 5-6, 427.

17. Klobuchar J.A., J. Aarons, E.J. Weber, R. Lucena, and M. Mendillo, 1978, URSI abstract, Boulder, Co.

18. Maeda H., 1955, Rept. Jonos. Res. Japan, 9, 59.

19. Maeda K., H. Uyeda, and H. Shinkawa, 1942, Res. Rept. Phys. Inst. Radio Waves, Ministry of Education, Japan.

20. Martyn D.F., 1947, Proc. Royal Soc. London, A189, 241.

21. Matsushita S., B.B. Balsley, and H. Rishbeth (editors), 1981, Equatorial Aeronomy I and II Special Issue of J. Atmospheric Terrest. Phys. 43, 516.

22. McClinton A.T., 1972, "USNS Hayes (T-AGOR-16) U.S. Navy Oceanographic Research Ship," NRL Report 7370.

23. Narcisi R.S. and E.P. Szuszczewicz, 1981, J. Atmospheric Terrest. Phys., 43 (5/6) 463-471.

24. Ossakow S.L., 1979, Rev. Geophys. Space Phys., 17, 521.

25. Ossakow S.L., 1981, J. Atmospheric Terrest. Phys., 43 (5/6) 437-452.

26. Rishbeth H., 1981, J. Atmos. Terr. Phys., 43, 5-6, 387.

27. Rishbeth H., 1971, Planet. Space Sci., 19, 263.

28. Szuszczewicz E.P., R.T. Tsunoda, R.S. Narcisi, and J.C. Holmes, 1980, Geophys. Res. Lett., 7, 537.

29. URSI Conference Proceedings, 1981, Washington, D. C.

30. Vasil'yer K.N., O.P. Kolomiytsev, and I.S. Poutanskiy, 1979, *Geomag.* and Aeron. 19 (2) 149.

31. Walton E.K., and S.K. Bowhill, 1979, J. Atmospheric Terrest. Phys. 41, 937.

32. Yeh K.C., H. Soicher, and C.H. Liu, 1979, J. Geophys. Res., 84, 6589.

DATE
ILME